Sustained Suppression of Neointimal Proliferation by Sirolimus-Eluting Stents

One-Year Angiographic and Intravascular Ultrasound Follow-Up

J. Eduardo Sousa, MD, PhD; Marco A. Costa, MD, PhD; Alexandre C. Abizaid, MD, PhD; Benno J. Rensing, MD, PhD; Andrea S. Abizaid, MD; Luiz F. Tanajura, MD; Ken Kozuma, MD; Glenn Van Langenhove, MD, PhD; Amanda G.M.R. Sousa, MD, PhD; Robert Falotico, PhD; Judith Jaeger, BA; Jeffrey J. Popma, MD; Patrick W. Serruys, MD, PhD

Background—We have previously reported a virtual absence of neointimal hyperplasia 4 months after implantation of sirolimus-eluting stents. The aim of the present investigation was to determine whether these results are sustained over a period of 1 year.

Methods and Results—Forty-five patients with de novo coronary disease were successfully treated with the implantation of a single sirolimus-eluting Bx VELOCITY stent in São Paulo, Brazil (n=30, 15 fast release [group I, GI] and 15 slow release [GII]) and Rotterdam, The Netherlands (15 slow release, GIII). Angiographic and volumetric intravascular ultrasound (IVUS) follow-up was obtained at 4 and 12 months (GI and GII) and 6 months (GIII). In-stent minimal lumen diameter and percent diameter stenosis remained essentially unchanged in all groups (at 12 months, GI and GII; at 6 months, GIII). Follow-up in-lesion minimal lumen diameter was 2.28 mm (GIII), 2.32 mm (GI), and 2.48 mm (GII). No patient approached the ≥50% diameter stenosis at 1 year by angiography or IVUS assessment, and no edge restenosis was observed. Neointimal hyperplasia, as detected by IVUS, was virtually absent at 6 months (2±5% obstruction volume, GIII) and at 12 months (GI=2±5% and GII=2±3%).

Conclusions—This study demonstrates a sustained suppression of neointimal proliferation by sirolimus-eluting Bx VELOCITY stents 1 year after implantation. (***Circulation.*** **2001;104:2007-2011.)**

Key Words: angiography ■ drugs ■ stents ■ restenosis ■ ultrasonics

Despite major technological advances in the past decades, of which the coronary stent is one of the most important, the percutaneous treatment of coronary artery disease is still hampered by a 20% to 30% incidence of restenosis. The list of candidate therapies and devices for prevention of restenosis after angioplasty is long and ever expanding. However, few if any have substantially improved the result of stenting for the treatment of de novo lesions. Intracoronary radiation has so far proven to be effective for the treatment of in-stent restenosis but not for the treatment of de novo lesions.[1] As a result of their ability to deliver prolonged and sufficient intramural drug concentrations to the target coronary segment, drug-eluting stents have emerged as a potential solution for restenosis. Our group has recently reported an almost complete absence of neointimal hyperplasia 4 months after implantation of sirolimus-eluting Bx VELOCITY stents.[2] The local release of sirolimus (rapamycin, Rapamune), a natural macrocyclic lactone with potent immunosuppressive action,[3] resulted in elimination of restenosis in this first series of patients. Comparable results have only been observed after the implantation of high-activity β-emitting stents (9 mm^3 of neointimal hyperplasia at 6-month follow-up).[4] However, a worrying late progression of in-stent neointimal hyperplasia was observed between 6 months and 1 year after implantation of radioactive stents.[5]

See p 1996

The aim of the present investigation was to determine whether sirolimus-eluting stents produce a sustained suppression of the neointimal proliferation over a period of 1 year or merely delay the restenosis process.

Methods

Study Population

Forty-five patients with native coronary artery disease and angina pectoris were successfully treated with the implantation of a single

Received July 10, 2001; revision received August 14, 2001; accepted August 15, 2001.

From the Institute Dante Pazzanese of Cardiology (J.E.S., M.A.C., A.C.A., A.S.A., L.F.T., A.G.M.R.S.), São Paulo, Brazil; Thoraxcenter, Dijkzigt University Hospital (B.J.R., K.K., G.V.L. P.W.S.), Rotterdam, The Netherlands; Cordis, a Johnson and Johnson Company (R.F., J.J.), Warren, NJ; and Brigham and Women's Hospital (J.J.P.), Boston, Mass.

Correspondence to Professor J. Eduardo Sousa, MD, PhD, Director of the Institute Dante Pazzanese of Cardiology, Av. Dr Dante Pazzanese, 500 - Ibirapuera, 04012180, São Paulo, Brazil. E-mail jesousa@uol.com.br

Circulation **is available at http://www.circulationaha.org**

sirolimus-eluting Bx VELOCITY stent. Only lesions ≤18 mm in length and vessels ≥3 and ≤3.5 mm in diameter were included. Total occlusion, ostial or thrombus containing lesions, unprotected left main disease with >50% stenosis, occurrence of myocardial infarction within the preceding 72 hours, and left ventricular ejection fraction <30% were the major exclusion criteria. Thirty patients were electively treated with two different formulations of sirolimus-eluting stents (fast release [FR], n=15, group I, and slow release [SR], n=15, group II) at the Institute Dante Pazzanese of Cardiology, São Paulo, Brazil. A third cohort of patients (n=15, group III) was treated with SR sirolimus-eluting stents at the Thoraxcenter, Erasmus University Rotterdam, The Netherlands.

Drug-Polymer Matrix and Elution Kinetics

Sirolimus was blended in a mixture of nonerodable polymers, and a 5-μm-thick layer of sirolimus-polymer matrix was applied onto the surface of the Bx VELOCITY stent (Cordis), a laser-cut 316L stainless-steel balloon-expandable stent.

The drug is almost completely eluted by 15 days after implantation in the FR formulation. Another layer of drug-free polymer was applied on top of the drug-polymer matrix to introduce a diffusion barrier and prolong drug release to >28 days in the SR formulation. All stents, regardless of the coating composition, were loaded with a fixed amount of sirolimus per unit of metal surface area (140 μg sirolimus/cm^2).

In vivo experiments have shown that sirolimus levels in whole blood peak at 1 hour (2.6±0.7 ng/mL, FR; 0.9±0.2 ng/mL, SR) after implantation and fall below the lower limit of quantification by 72 hours (0.4 ng/mL) (Bruce D. Klugherz, unpublished data, 2000). Taking into account that renal transplant patients maintain chronic blood levels of rapamycin between 8 and 17 ng/mL, the peak blood level after implantation of a sirolimus-eluting stent is absolutely negligible.

Stent Procedure

Stents were implanted according to standard practice, after balloon predilatation and followed by high-pressure (>12 atmospheres) balloon after dilatation. All stents were 18 mm long and 3 to 3.5 mm in diameter. Heparin was given to maintain the activated clotting time >300 seconds. Patients received aspirin (325 mg/d, indefinitely) started at least 12 hours before the procedure and a 300-mg loading dose of clopidogrel immediately after stent implantation and 75 mg/d for 60 days. The protocol was approved by the Medical Ethical Committees of both institutions, and written informed consent was obtained from every patient.

Angiographic and IVUS Procedures

Patients in São Paulo (groups I and II) underwent intravascular ultrasound (IVUS) and angiographic follow-up at 4 and 12 months. In Rotterdam (group III), patients returned for repeat angiography and IVUS assessment at 6 months, the classical restenosis time point. Intracoronary nitrates were administered immediately before each angiographic and IVUS acquisition. Postprocedure angiography was performed in at least 2 orthogonal projections, which were repeated at the follow-up studies. Quantitative angiographic analysis was done by an independent core laboratory (Brigham and Women's Hospital, Boston, Mass).

The segments subject to three-dimensional (3D) IVUS reconstruction were examined with a 30-MHz single-element mechanical transducer (ClearView, CVIS, Boston Scientific Corporation). A constant pullback speed of 0.5 mm/s was used for IVUS image acquisitions. A complete IVUS run was recorded on s-VHS tape for offline 3D reconstruction. At 12 months, IVUS images were also acquired using an ECG-triggered pullback device with a stepping motor at 0.2 mm/step (EchoScan, Tomtec) to assure a precise quantification of neointimal hyperplasia volume. This system acquires images coinciding with the peak of the R wave, eliminating the artifacts caused by the movement of the heart during the cardiac cycle and ultimately improving the quality of image for 3D volumetric quantification. Volumetric IVUS analysis was carried out by an independent core laboratory (Cardialysis BV, Rotterdam, The Netherlands).[6,7]

Quantitative Measurements

Two coronary segments were subjected to quantitative angiography, in-stent and in-lesion segments. The in-stent analysis encompassed only the 18-mm-long segment covered by the stent. The in-lesion segment was defined as the stent plus 5 mm proximal and 5 mm distal to the edge or the nearest side branch. In-stent and in-lesion restenosis was defined as ≥50% diameter stenosis (DS) at follow-up, located within the stent and target lesion, respectively. Edge restenosis was defined as ≥50% DS at follow-up, located at the proximal or distal edge. Minimal lumen diameter (MLD) and percent DS were calculated for each segment.

Quantitative IVUS analyses of the stent segment were performed at all time points. Lumen and stent boundaries were detected using a minimum-cost algorithm. Total stent and lumen volumes were calculated as previously described. Intimal hyperplasia (IH) volume was calculated as stent volume minus luminal volume. Feasibility, reproducibility, and interobserver and intraobserver variability of these measurements have been validated previously.[8]

Statistical Analysis

Continuous variables are expressed as mean±SD. Comparisons between postintervention and follow-up measurements were performed with a 2-tailed paired *t* test. Comparisons between groups were performed using unpaired Student's *t* test. A *P* value <0.05 was considered statistically significant.

Results

Baseline characteristics were similar between the 3 groups. Overall, 29 patients were male, 32 had stable angina, and 13 were unstable. Mean age was 55.1 (group I), 57.9 (group II) and 60 years (group III). Six patients had a history of diabetes mellitus. Clopidogrel was discontinued at 60 days in all patients.

At the Thoraxcenter, 1 of the 15 patients died on day 2 of a cerebral hemorrhage. She had received abciximab during the procedure and for 12 hours thereafter. Two additional patients (group III) suffered a vessel occlusion during or immediately after the procedure attributable to distal edge dissection and were successfully treated with additional stenting. Subsequent clinical follow-up was uneventful for both patients, and no restenosis was detected at 6-month angiographic follow-up. Finally, 1 asymptomatic patient from Rotterdam refused repeat angiography; thus, 13 completed 6-month angiographic and IVUS follow-up. As reported previously,[2] all patients in groups I and II were discharged without any clinical event. One asymptomatic patient (group II) refused repeat angiography at 12 months.

A representative sequence of angiograms from a single patient are shown in Figure 1. Preprocedure reference vessel diameter (RD) was 2.85±0.46 mm, and postprocedure MLD was 2.47±0.38-mm (in-lesion) and 2.9±0.27-mm (in-stent) in the Rotterdam patients (group III). Four-month data from groups I and II have been reported previously.[2] One-year in-stent MLD (group I, 2.73±0.3 mm; group II, 2.87±0.4 mm) and percent DS (group I, 8.9±6.1%; group II, 6.7±7%) remained essentially unchanged compared with 4-month follow-up. At 6 months (group III), in-stent MLD was 2.66±0.3 mm, and percent DS was 8.9±7.6% (*P*=NS compared with postprocedure) Changes in in-lesion MLD and percent DS are shown in Figure 2. At 12 months,

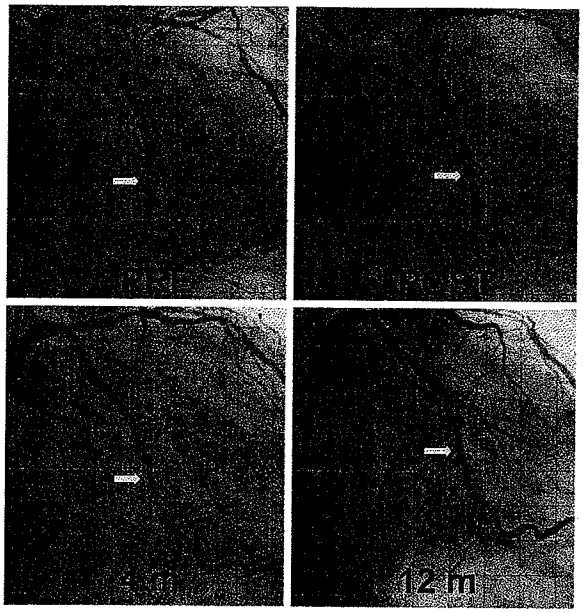

Figure 1. Angiography shows a lesion in the mid portion of the left circumflex marginal branch (white arrow), which was treated with the implantation of a sirolimus-coated BX-velocity stent (top right). Lumen dimensions remained unchanged at 4- and 12- month follow-up (bottom).

in-lesion angiographic lumen dimension showed a small decrease compared with postprocedure in both groups (Figure 2, $P<0.01$). Between 4 months and 12 months, a very small decrease, albeit statically significant ($P=0.004$), in in-lesion MLD was observed in group I. No patient approached the ≥50% DS at 1-year by angiography or IVUS assessment, and no edge restenosis was observed.

At 6-month follow-up, lumen volume was 156.7±63.6 mm^3 (versus 156.5±64.1 mm^3 at postprocedure, P=NS) and intimal hyperplasia volume was 5.7±17.7 mm^3 (group III). Thus, the percent obstruction volume was 2±4.98%, similar to the results reported at 4 months in the patients from São Paulo.[2]

One-year volumetric IVUS data (Figure 3) from the São Paulo patients were actually better than those reported previously at 4-month follow-up.[2] Only 2 patients had >10% IH after 12 months (Figure 3). Differences in the method of volumetric quantification probably explain these findings. As

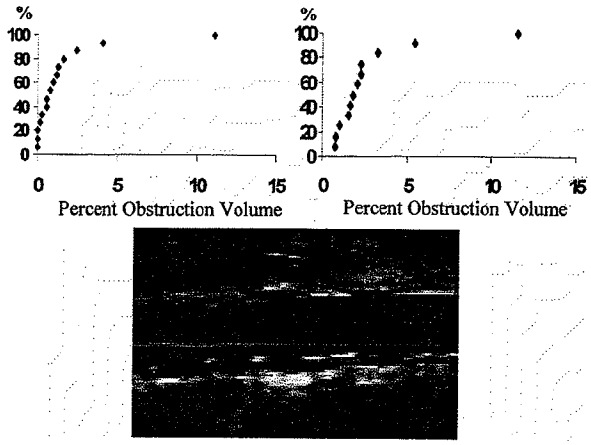

Figure 3. Cumulative distribution curves of percent obstruction volumes in group I (left) and group II (right) at 12-month follow-up. Longitudinal IVUS reconstruction illustrates the virtual absence of in-stent intimal hyperplasia at 12 months (bottom).

a result of the virtual absence of neointimal hyperplasia, the automated contour detection algorithm that was used for the original analysis superimposed the contours of the stent and lumen boundaries in the majority of the cases. Thus, the core laboratory analyst used a "copy and shrink" tool of the quantitative analysis software to dissociate the two contours. This action led to an overestimation of the amount of IH. At 12-month follow-up analysis, the lumen and stent contours were not dissociated artificially, unless IH was clearly visualized. To compare 4-month and 12-month IVUS data, the core laboratory reanalyzed the 4-month IVUS images using the same methodology used at 12 months (Table).

In one patient (group I), 12-month IVUS assessment showed an unstable plaque proximal to the stent. Lesion vulnerability was characterized by positive vessel remodeling and a large lipid pool delimited by a thin fibrous cap (Figure 4). This preexisting plaque increased progressively from the time of the initial procedure, producing a linear deterioration in lumen dimensions (MLD was 2.85 mm postprocedure, 2.51 mm at 4 months, and 2.02 mm at 12 months). No sign of thrombus was detected by angiography or IVUS. At 12 months, the patient was asymptomatic and had a negative stress test. However, at 14-month follow-up, he returned with a non–Q-wave myocardial infarction. Angiography showed

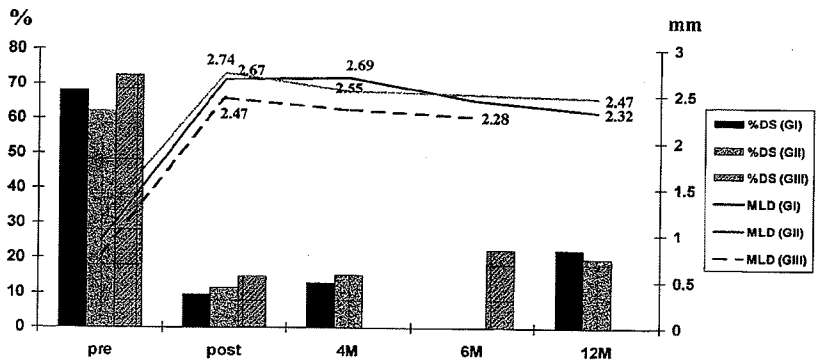

Figure 2. In-lesion percent diameter stenosis (%DS) and MLD over a period of 1 year. Angiographic follow-up was performed at 4 and 12 months in group I (GI) and GII and at 6 months in GIII.

Three-Dimensional Volumetric IVUS Measurements 4 and 12 Months After Implantation of Sirolimus-Eluting Stent

	Stent Volume, mm^3		Lumen Volume, mm^3		IH Volume, mm^3		Obstruction Volume, %	
Follow-up period, mo	4	12	4	12	4	12	4	12
Group I	134±30	127±26	134±30	124±25	0.4±0.8	3.2±8.5	0.3±0.6	2.3±5.5
Group II	138±21	127±30	137±22	124±30	0.3±0.9	2.5±3.4	0.3±0.8	2.2±3.4

No statistical differences were observed between groups or between 4-month and 12-month data within the same group.

the target vessel occluded proximal to the stent, and repeat angioplasty was performed.

The remaining 29 patients of the first 2 cohorts (groups I and II) have now completed 15-month clinical follow-up uneventfully. Similarly, the 14 Rotterdam patients were asymptomatic, with no additional adverse events up to 9 months after the index procedure.

Discussion

The present study demonstrates a potent, long-lasting inhibitory effect on neointimal proliferation exerted by the local release of sirolimus via a stent platform. Regardless of the coating formulation (SR or FR) or population treated (São Paulo or Rotterdam), neointimal hyperplasia, as detected by both angiography and volumetric IVUS quantification, was minimal at all time points (4, 6, or 12 months).

The lack of restenosis observed in this first series of patients treated with sirolimus-eluting Bx VELOCITY stents is probably a consequence of the scaffolding properties of the stent as well as the potent cytostatic effect of sirolimus.[9,10] Like cyclosporin A and tacrolimus (FK506), sirolimus binds to specific cytosolic proteins. However, the mechanism of action of sirolimus is distinct from other immunosuppressive agents that act solely by inhibiting DNA synthesis. The sirolimus:FKBP complex binds to a specific cell-cycle regulatory protein, the mTOR (mammalian target of rapamycin), and inhibits its activation.[11] The inhibition of mTOR induces cell-cycle arrest in late G1 phase.[12–14] The upregulation of FK506-binding protein 12 (FKBP12) observed in human neointimal smooth muscle cells additionally supports the potential antirestenotic effect of sirolimus.[15] Preclinical data have demonstrated the efficacy of both systemic[13,16] and local administration (via drug-eluting stent) (Andrew J. Carter, unpublished data, 2000) of sirolimus in reducing neointimal hyperplasia in different models of restenosis.

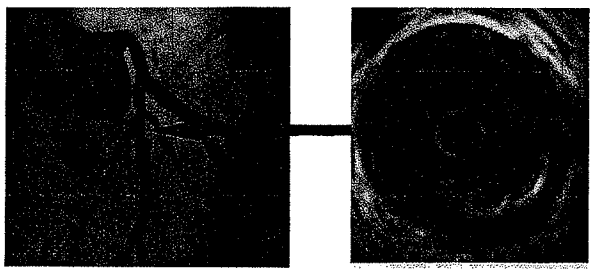

Figure 4. Angiography of the left anterior descending artery showing a nonsignificant stenosis at the proximal edge of the stent (white arrow) at 12-month follow-up. IVUS cross-sectional image at the site of the lesion shows an eccentric plaque with a large lipid pool (L) delimitated by a fibrous cap (arrows). This vessel was occluded 2 months later.

A concern about potential late complications, such as late thrombosis, associated with new therapies is a legacy from our previous experience with intracoronary radiation therapy.[17] In our series, one patient (out of 44) experienced a thrombotic event involving the target coronary artery 14 months after the procedure. It is important to note that IVUS showed an unstable plaque located proximal to the stent that grew progressively in size over the period of observation. The relationship between unstable plaque, as characterized by IVUS, and coronary thrombosis has been reported previously and may explain this unexpected event.[18,19] Experimental investigations have shown a similar degree of re-endothelialization between bare and sirolimus-coated stents occurring as early as 30 days after implantation (Andrew J Carter, unpublished data, 2001), ie, sirolimus does not seem to delay endothelialization. Nevertheless, one cannot completely rule out the possibility of late-stent thrombosis as a cause of vessel occlusion in this case. The occurrence of this somewhat anecdotal event should be interpreted with caution. Data from large randomized multicenter trials, already underway, will be necessary to definitively address this important question.

After our previous study showing a surprising near-absence of IH 4 months after implantation of sirolimus-eluting stents,[2] the logical question was whether this effect would be permanent or whether it merely represented a delay in the proliferative response. The basis for these concerns is the unexpected late-luminal deterioration observed with catheter-based radiation systems and radioactive stents,[1,5] although the mechanisms of action of sirolimus-eluting stents differ considerably from intracoronary brachytherapy. In the present study, angiographic lumen dimensions and IVUS-detected IH volume assessed both at 6-month follow-up (in group III) and at 12 months (groups I and II) was not substantially different from what was observed at 4 months (Table). Thus, at 12-month follow-up, there is no evidence of significant late catch up, and the 12-month IH volume observed in the present study is less than one third of that reported with any previously tested antirestenosis therapy.[6,7] If the findings of the present investigation are confirmed by large, randomized, placebo-controlled trials, this technology is likely to have a major impact on the treatment of coronary artery disease in the near future.

Acknowledgments

We are indebted to the patients for their participation in this research. We gratefully appreciate the invaluable contribution of the medical and technical staffs of the Institute Dante Pazzanese of Cardiology

and Thoraxcenter. We also thank Dr Brian Firth for his careful review of the manuscript and constructive comments.

References

1. Teirstein PS, Massullo V, Jani S, et al. Two-year follow-up after catheter-based radiotherapy to inhibit coronary restenosis. *Circulation*. 1999;99:243–247.
2. Sousa JE, Costa MA, Abizaid A, et al. Lack of neointimal proliferation after implantation of sirolimus-coated stents in human coronary arteries: a quantitative coronary angiography and three-dimensional intravascular ultrasound study. *Circulation*. 2001;103:192–195.
3. Groth CG, Backman L, Morales JM, et al. Sirolimus (rapamycin)-based therapy in human renal transplantation: similar efficacy and different toxicity compared with cyclosporine. Sirolimus European Renal Transplant Study Group. *Transplantation*. 1999;67:1036–1042.
4. Kay IP, Sabate M, Costa MA, et al. Positive geometric vascular remodeling is seen after catheter-based radiation followed by conventional stent implantation but not after radioactive stent implantation. *Circulation*. 2000;102:1434–1439.
5. Kay IP, Wardeh AJ, Kozuma K, et al. Radioactive stents delay but do not prevent in-stent neointimal hyperplasia. *Circulation*. 2001;103:14–17.
6. Acute platelet inhibition with abciximab does not reduce in-stent restenosis (ERASER study): the ERASER Investigators. *Circulation*. 1999; 100:799–806.
7. Costa MA, Sabaté M, Kay IP, et al. Three-dimensional intravascular ultrasonic volumetric quantification of stent recoil and neointimal formation of two new generation tubular stents. *Am J Cardiol*. 2000;85: 135–139.
8. von Birgelen C, de Vrey EA, Mintz GS, et al. ECG-gated three-dimensional intravascular ultrasound: feasibility and reproducibility of the automated analysis of coronary lumen and atherosclerotic plaque dimensions in humans. *Circulation*. 1997;96:2944–2952.
9. Poon M, Marx SO, Gallo R, et al. Rapamycin inhibits vascular smooth muscle cell migration. *J Clin Invest*. 1996;98:2277–2283.
10. Gonzalez J, Harris T, Childs G, et al. Rapamycin blocks il-2-driven t cell cycle progression while preserving t cell survival. *Blood Cells Mol Dis*. 2001;27:572–585.
11. Roque M, Reis ED, Cordon-Cardo C, et al. Effect of p27 deficiency and rapamycin on intimal hyperplasia: in vivo and in vitro studies using a p27 knockout mouse model. *Lab Invest*. 2001;81:895–903.
12. Roque M, Cordon-Cardo C, Fuster V, et al. Modulation of apoptosis, proliferation, and p27 expression in a porcine coronary angioplasty model. *Atherosclerosis*. 2000;153:315–322.
13. Gallo R, Padurean A, Jayaraman T, et al. Inhibition of intimal thickening after balloon angioplasty in porcine coronary arteries by targeting regulators of the cell cycle. *Circulation*. 1999;99:2164–2170.
14. Marx SO, Jayaraman T, Go LO, et al. Rapamycin-FKBP inhibits cell cycle regulators of proliferation in vascular smooth muscle cells. *Circ Res*. 1995;76:412–417.
15. Zohlnhofer D, Klein CA, Richter T, et al. gene expression profiling of human stent-induced neointima by cDNA array analysis of microscopic specimens retrieved by helix cutter atherectomy: detection of FK506-binding protein 12 upregulation. *Circulation*. 2001;103:1396–1402.
16. Gregory CR, Huie P, Billingham ME, et al. Rapamycin inhibits arterial intimal thickening caused by both alloimmune and mechanical injury: its effect on cellular, growth factor, and cytokine response in injured vessels. *Transplantation*. 1993;55:1409–1418.
17. Costa MA, Sabate M, van der Giessen WJ, et al. Late coronary occlusion after intracoronary brachytherapy. *Circulation*. 1999;100:789–792.
18. Ge J, Chirillo F, Schwedtmann J, et al. Screening of ruptured plaques in patients with coronary artery disease by intravascular ultrasound. *Heart*. 1999;81:621–627.
19. Schoenhagen P, Ziada KM, Kapadia SR, et al. Extent and direction of arterial remodeling in stable versus unstable coronary syndromes: an intravascular ultrasound study. *Circulation*. 2000;101:598–603.

ORIGINAL CONTRIBUTION

Comparison of an Everolimus-Eluting Stent and a Paclitaxel-Eluting Stent in Patients With Coronary Artery Disease

A Randomized Trial

Gregg W. Stone, MD
Mark Midei, MD
William Newman, MD
Mark Sanz, MD
James B. Hermiller, MD
Jerome Williams, MD
Naim Farhat, MD
Kenneth W. Mahaffey, MD
Donald E. Cutlip, MD
Peter J. Fitzgerald, MD, PhD
Poornima Sood, MD, MPhil
Xiaolu Su, MS
Alexandra J. Lansky, MD
for the SPIRIT III Investigators

Context A thin, cobalt-chromium stent eluting the antiproliferative agent everolimus from a nonadhesive, durable fluoropolymer has shown promise in preliminary studies in improving clinical and angiographic outcomes in patients with coronary artery disease.

Objective To evaluate the safety and efficacy of an everolimus-eluting stent compared with a widely used paclitaxel-eluting stent.

Design, Setting, and Patients The SPIRIT III trial, a prospective, randomized, single-blind, controlled trial enrolling patients at 65 academic and community-based US institutions between June 22, 2005, and March 15, 2006. Patients were 1002 men and women undergoing percutaneous coronary intervention in lesions 28 mm or less in length and with reference vessel diameter between 2.5 and 3.75 mm. Angiographic follow-up was prespecified at 8 months in 564 patients and completed in 436 patients. Clinical follow-up was performed at 1, 6, 9, and 12 months.

Interventions Patients were randomized 2:1 to receive the everolimus-eluting stent (n=669) or the paclitaxel-eluting stent (n=333).

Main Outcome Measures The primary end point was noninferiority or superiority of angiographic in-segment late loss. The major secondary end point was noninferiority assessment of target vessel failure events (cardiac death, myocardial infarction, or target vessel revascularization) at 9 months. An additional secondary end point was evaluation of major adverse cardiac events (cardiac death, myocardial infarction, or target lesion revascularization) at 9 and 12 months.

Results Angiographic in-segment late loss was significantly less in the everolimus-eluting stent group compared with the paclitaxel group (mean, 0.14 [SD, 0.41] mm vs 0.28 [SD, 0.48] mm; difference, −0.14 [95% CI, −0.23 to −0.05]; $P \leq .004$). The everolimus stent was noninferior to the paclitaxel stent for target vessel failure at 9 months (7.2% vs 9.0%, respectively; difference, −1.9% [95% CI, −5.6% to 1.8%]; relative risk, 0.79 [95% CI, 0.51 to 1.23]; $P < .001$). The everolimus stent compared with the paclitaxel stent resulted in significant reductions in composite major adverse cardiac events both at 9 months (4.6% vs 8.1%; relative risk, 0.56 [95% CI, 0.34 to 0.94]; $P = .03$) and at 1 year (6.0% vs 10.3%; relative risk, 0.58 [95% CI, 0.37 to 0.90]; $P = .02$), due to fewer myocardial infarctions and target lesion revascularization procedures.

Conclusions In this large-scale, prospective randomized trial, an everolimus-eluting stent compared with a paclitaxel-eluting stent resulted in reduced angiographic late loss, noninferior rates of target vessel failure, and fewer major adverse cardiac events during 1 year of follow-up.

Trial Registration clinicaltrials.gov Identifier: NCT00180479

JAMA. 2008;299(16):1903-1913 www.jama.com

BY ENLARGING THE ARTERIAL lumen and sealing dissection planes, stent implantation relieves coronary flow obstruction at the site of atherosclerotic disease. However, injury to the tunica media results in excessive neointimal hyperplasia in approximately 20% to 30% of patients treated with bare-metal stents, which results in recurrent ischemia often necessitating rehospitalization for repeat percutaneous coronary intervention or coronary artery bypass graft surgery.[1] Drug-eluting stents combine the mechanical scaffolding properties of metallic stents with the site-specific delivery of an antiproliferative agent designed to inhibit vascular responses to arterial injury, thereby reducing restenosis. The polymer-regulated, site-specific delivery of paclitaxel and sirolimus have been shown to inhibit tissue growth after coronary stent implantation and to improve long-term event-free survival compared with bare-metal stents.[2,3] However, restenosis still occurs, and the incidence of stent thrombosis, especially after

For editorial comment see p 1952.

Author Affiliations and a List of the SPIRIT III Investigators appear at the end of this article.
Corresponding Author: Gregg W. Stone, MD, Columbia University Medical Center, The Cardiovascular Research Foundation, 111 E 59th St, 11th Floor, New York, NY 10022 (gs2184@columbia.edu).

the first year of implantation, is increased with these drug-eluting stents compared with their bare-metal counterparts,[4,5] likely due to delayed and incomplete endothelialization.[6,7]

Newer drug-eluting stents are being designed with the goal of enhanced safety, efficacy, or both compared with previous devices. Everolimus, a semisynthetic macrolide immunosuppressant, is an analogue of rapamycin, which binds to cytosolic FKBP12 and subsequently to the mammalian target of rapamycin, thereby blocking the stimulatory effects of growth factors and cytokines, which are released after vascular injury. As a result, cell cycle progression is blocked between the G1 and S phases, inhibiting smooth muscle cell proliferation.[8]

Everolimus has been shown to prevent cardiac allograft vasculopathy,[9] which histologically resembles the neointimal hyperplasia that develops after coronary stent implantation.[10] An everolimus-eluting stent has been designed in which the drug is released from a thin (7.8-μm), nonadhesive, durable, biocompatible fluoropolymer coated onto a low-profile (0.0032-in [0.0813-mm] strut thickness), flexible cobalt-chromium stent. Preclinical studies have shown more rapid endothelialization with this stent compared with sirolimus-eluting and paclitaxel-eluting stents.[11] Following favorable results with this device in 1 small and 1 moderate-sized randomized study in Europe,[12,13] the large-scale SPIRIT III trial was performed to evaluate the everolimus-eluting stent in comparison to a widely used paclitaxel-eluting stent in patients with coronary artery disease.

METHODS

Study Population, Device Description, and Protocol

SPIRIT III was a prospective, multicenter, randomized, single-blind, controlled clinical trial in which 1002 patients with either 1 or 2 de novo native coronary artery lesions (maximum 1 lesion per epicardial coronary artery) were randomized in a 2:1 ratio to receive the polymer-based everolimus-eluting stent (XIENCE V; Abbott Vascular, Santa Clara, California) or the polymer-based paclitaxel-eluting stent (TAXUS EXPRESS2; Boston Scientific, Natick, Massachusetts). Patients aged 18 years or older with stable or unstable angina or inducible ischemia undergoing percutaneous coronary intervention were considered for enrollment.

Clinical exclusion criteria included percutaneous intervention in the target vessel either prior to or planned within 9 months after the index procedure; intervention in a nontarget vessel within 90 days prior to or planned within 9 months after the index procedure; prior coronary brachytherapy at any time; acute or recent myocardial infarction with elevated cardiac biomarker levels; left ventricular ejection fraction less than 30%; prior or planned organ transplantation; current or planned chemotherapy for malignancy; known immunologic or autoimmune disease or prescribed immunosuppressive medication; use of chronic anticoagulation; contraindications or allergy to aspirin, heparin, and bivalirudin, thienopyridines, everolimus, cobalt, chromium, nickel, tungsten, acrylic, or fluoropolymers, or to iodinated contrast that cannot be premedicated; elective surgery planned within 9 months after the procedure, necessitating antiplatelet agent discontinuation; platelet count less than 100 000 cells/μL or greater than 700 000 cells/μL, white blood cell count less than 3000 cells/μL, serum creatinine level greater than 2.5 mg/dL (to convert to μmol/L, multiply by 88.4), or dialysis or liver disease; recent major bleeding, hemorrhagic diathesis, or objection to blood transfusions; stroke or transient ischemic attack within 6 months; comorbid conditions that limit life expectancy to less than 1 year or that could affect protocol compliance; positive pregnancy test result, lactation, or planned pregnancy within 1 year after enrollment; and participation in another investigational study that has not yet reached its primary end point. The study was approved by the institutional review board at each participating center, and consecutive, eligible patients signed written informed consent.

Prior to catheterization, an electrocardiogram was performed, creatine phosphokinase and isoenzyme levels were measured, and 300 mg or more of aspirin was administered. A 300-mg or greater oral dose of clopidogrel was recommended preprocedure and required in all cases within 1 hour after stent implantation. Procedural anticoagulation was achieved with either unfractionated heparin or bivalirudin per standard of care, and use of glycoprotein IIb/IIIa inhibitors was per operator discretion. Angiographic eligibility was assessed following mandatory predilatation. The reference vessel diameter of all study lesions was required to be between 2.5 mm and 3.75 mm, and the lesion length was required to be 28 mm or less, both by visual assessment, representing the on-label lesion dimensions for which the paclitaxel-eluting stent has been approved by the US Food and Drug Administration (FDA) for use in the United States. Other angiographic exclusion criteria included ostial or left main lesions; bifurcation lesions with either side branch more than 50% stenosed or more than 2 mm in diameter or requiring predilatation; excessive proximal tortuosity, lesion angulation or calcification, or thrombus; lesion located within a bypass graft conduit; diameter stenosis less than 50% or 100%, or the presence of lesions with greater than 40% stenosis within the target vessel or likelihood that additional percutaneous intervention would be required within 9 months.

Following confirmation of angiographic eligibility, telephone randomization was performed in randomly alternating blocks of 3 and 6 patients using an automated voice response system, stratified by the presence of diabetes, planned dual-vessel treatment, and study site. For this trial everolimus-eluting stents were available in 2.5-, 3.0-, and 3.5-mm diameters, and in 8-, 18-, and 28-mm lengths. The full range of US-manufactured paclitaxel-eluting stents were available, ranging from 2.5 to 3.5 mm in diameter and from 8 to 32 mm in length. An appropriate-length stent was selected sufficient to cover approximately 3 mm of nondiseased tissue on either side of the lesion. In patients receiving multiple

stents for a single lesion, 1 to 4 mm of stent overlap was recommended. Additional study stents were permitted for edge dissections greater than type C or otherwise suboptimal results, and postdilation was at operator discretion.

Following the procedure, an electrocardiogram was performed and cardiac enzyme levels were measured. The protocol recommended that patients receive aspirin (≥80 mg/d) indefinitely and clopidogrel (75 mg/d) for a minimum of 6 months. Clinical follow-up was scheduled at 30 (±7) days, 180 (±14) days, 240 (±28) days, 270 (±14) days, 365 (±28) days, and then yearly (±28 days) through 5 years. Although the operators were by necessity unblinded during the stent implantation procedure, the patient and staff involved in follow-up assessments remained blinded through the follow-up period, with a standardized follow-up interview script used to reduce bias. Protocol-specified angiographic follow-up was scheduled at 240 (±28) days in the first 564 patients enrolled. Among these patients, intravascular ultrasound immediately following stent implantation and at follow-up was intended in 240 patients at selected sites.

Data Management

Independent study monitors verified 100% of case report form data on-site. Data were stored in a database maintained by Abbott Vascular. All major adverse cardiac events were adjudicated by an independent committee blinded to treatment allocation after review of original source documentation. A second clinical events committee blinded to randomization performed a post hoc adjudication of stent thrombosis using the Academic Research Consortium definitions.[14] A data and safety monitoring board periodically reviewed blinded safety data, each time recommending that the study continue without modification. Independent core angiographic and intravascular ultrasound analyses were performed by technicians blinded to treatment assignment and clinical outcomes using validated methods as previously described.[15,16]

End Points and Definitions

The primary end point was in-segment late loss at 240 days (defined as the difference in the minimal luminal diameter assessed immediately after the pro-

Figure 1. Patient Flow and Follow-up in the SPIRIT III Trial

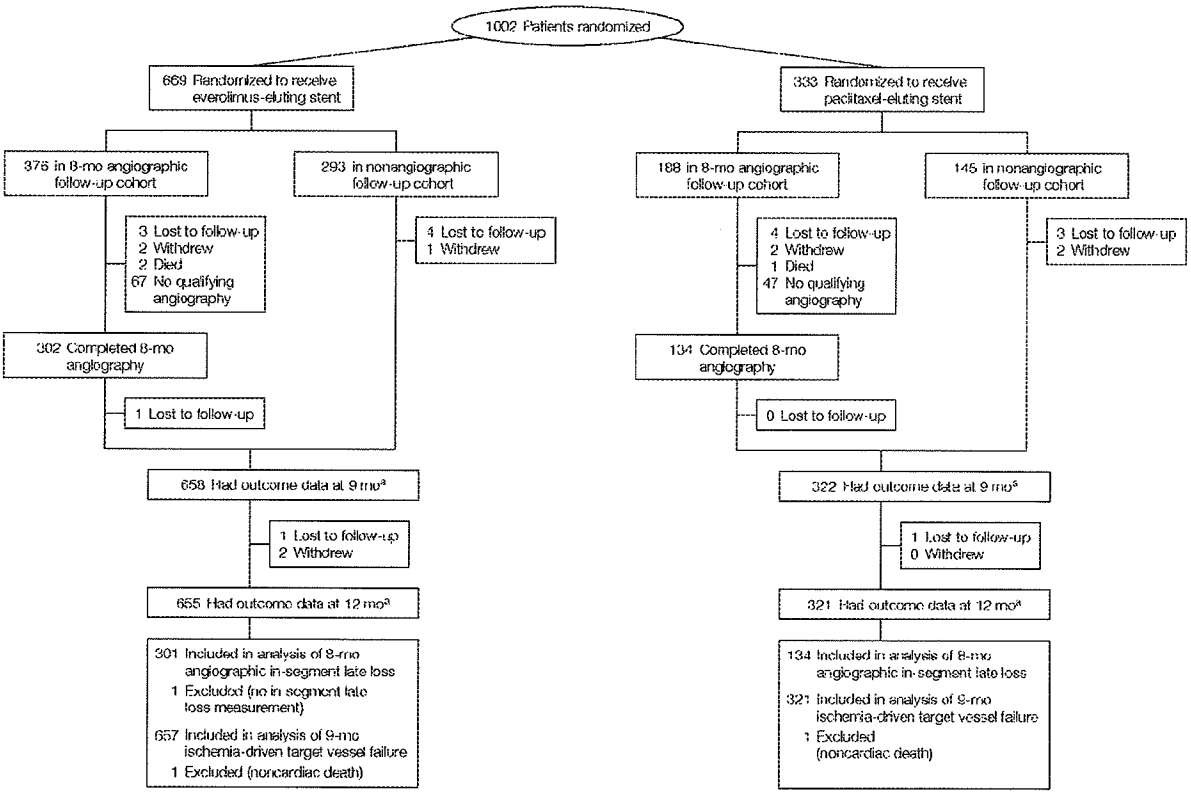

Prior to the 1-year follow-up period, 14 of 669 patients (2.1%) randomized to receive the everolimus-eluting stent either withdrew (n=5) or were lost to follow-up (n=9), and 12 of 333 patients (3.6%) randomized to receive the paclitaxel-eluting stent either withdrew (n=4) or were lost to follow-up (n=8).
[a]Nine-month follow-up was performed at 270 (±14) days; 12-month follow-up, at 365 (±28) days.

Table 1. Baseline Characteristics of the Study Population

Characteristic	Everolimus-Eluting Stent	Paclitaxel-Eluting Stent
Demographics, No./total (%)	669	332
Age, mean (SD), y	63.2 (10.5)	62.8 (10.2)
Men	469/669 (70.1)	218/332 (65.7)
Hypertension	510/669 (76.2)	245/331 (74.0)
Hypercholesterolemia	489/659 (74.2)	233/326 (71.5)
Diabetes mellitus		
Any	198/669 (29.6)	92/330 (27.9)
Requiring insulin	52/669 (7.8)	18/330 (5.5)
Current smoker	154/659 (23.4)	73/324 (22.5)
Prior myocardial infarction	130/652 (19.9)	59/327 (18.0)
Unstable angina	123/657 (18.7)	82/327 (25.1)
Target vessel, No./total (%)	772	383
Left anterior descending	317/768 (41.3)	164/382 (42.9)
Left circumflex	212/768 (27.6)	108/382 (28.3)
Right coronary	238/768 (31.0)	109/382 (28.5)
Left main, protected	1/768 (0.1)	1/382 (0.3)
Target lesion, mean (SD)	772	383
Reference vessel diameter, mm	2.77 (0.45)	2.76 (0.46)
Minimal luminal diameter, mm	0.82 (0.41)	0.83 (0.40)
Diameter stenosis, %	70.0 (13.3)	69.4 (13.6)
Lesion length, mm	14.7 (5.6)	14.7 (5.7)

cedure and at angiographic follow-up, measured within the margins, 5 mm proximal and 5 mm distal to the stent). To avoid interlesion clustering of restenosis in patients receiving stents for multiple lesions[17] (which would have required correction with multilevel generalized estimating equations), the protocol specified that for patients in whom 2 lesions were treated a single lesion (the analysis lesion) would be randomly selected by computer for analysis of late loss. All randomized lesions were included in the analyses for all other angiographic end points.

The major secondary end point was ischemia-driven target vessel failure at 270 days, defined as the composite of cardiac death (death in which a cardiac cause could not be excluded), myocardial infarction (Q-wave or non–Q-wave), and ischemia-driven target vessel revascularization by either percutaneous coronary intervention or bypass graft surgery. Target vessel (or lesion) revascularization was considered to be ischemia-driven if associated with a positive functional study result, a target vessel (or lesion) diameter stenosis of 50% or greater by core laboratory quantitative analysis with ischemic symptoms, or a target vessel (or lesion) diameter stenosis of 70% or greater with or without documented ischemia.

An additional prespecified secondary end point included major adverse cardiac events at 9 months and 1 year, defined as the composite of cardiac death, myocardial infarction, or ischemia-driven target lesion revascularization. Myocardial infarction was defined either as the development of new pathologic Q waves 0.4 seconds or longer in duration in 2 or more contiguous leads or as an elevation of creatine phosphokinase levels to more than 2 times normal with positive levels of creatine phosphokinase MB. Stent thrombosis was prospectively defined by protocol as an acute coronary syndrome with angiographic evidence of thrombus within or adjacent to a previously treated target lesion or, in the absence of angiography, as any unexplained death or acute myocardial infarction with ST-segment elevation or new Q waves in the distribution of the target lesion occurring within 30 days. Binary restenosis was defined as 50% or greater diameter stenosis of the treated lesion at angiographic follow-up. Other angiographic and intravascular ultrasound parameters were defined as previously described.[15,16]

Statistical Methods

The trial was powered for noninferiority for both the primary end point of in-segment late loss at 8 months among patients in the angiographic follow-up cohort, as well as the major secondary end point of ischemia-driven target vessel failure at 9 months in all enrolled patients. As agreed on with FDA, noninferiority for in-segment late loss would be declared if the upper limit of the 1-sided 97.5% confidence interval (CI) of the difference did not exceed a delta of 0.195 mm from the observed in-segment late lumen loss in the paclitaxel-eluting stent group, equivalent to a 1-sided test with $\alpha = .025$. Assuming a mean late loss of 0.24 (SD, 0.47) mm for both stents, with angiographic follow-up performed in 338 everolimus-eluting stent and 169 paclitaxel-eluting stent analysis lesions, the trial had 99% power to demonstrate noninferiority for in-segment late loss. Sequential superiority testing was prespecified if noninferiority for late loss was met. Noninferiority for ischemia-driven target vessel failure was declared if the upper limit of the 1-sided 95% CI of the difference did not exceed a delta of 5.5% from the observed paclitaxel-eluting stent control event rate. Assuming a target vessel failure rate of 9.4% for both stents, with 9-month clinical follow-up performed in 660 patients randomized to receive the everolimus-eluting stent and 330 to receive the paclitaxel-eluting stent, the trial had 89% power to demonstrate noninferiority for target vessel failure. Noninferiority for the prespecified powered primary as well as the major secondary end points had to be met for the trial to be considered successful, and as such both are considered coprimary end points.

Categorical variables were compared by Fisher exact test. Continuous variables are presented as mean (SD) and were compared by *t* test. The statistical analysis plan prespecified that all primary and secondary analyses

would be performed in the intent-to-treat population, consisting of all patients randomized in the study, regardless of the treatment actually received. However, patients lost to follow-up in whom no event had occurred prior to the follow-up windows were not included in the denominator for calculations of binary end points. Survival curves using all available follow-up data were also constructed for time-to-event variables using Kaplan-Meier estimates and compared by log-rank test. Superiority testing was performed after demonstration of noninferiority for the primary and major secondary end points[8] and for all other secondary end points using a 2-sided $\alpha = .05$. All statistical analyses were performed using SAS version 9.1.3 (SAS Institute Inc, Cary, North Carolina).

RESULTS

Patients and Enrollment

Between June 22, 2005, and March 15, 2006, 1002 patients were enrolled at 65 US sites and randomized to receive the everolimus-eluting stent (n=669) or the paclitaxel-eluting stent (n=333) (FIGURE 1). One patient in the paclitaxel group did not sign informed consent; thus, his or her data are unavailable. Baseline characteristics of the patients were well matched between the 2 groups (TABLE 1), except for slightly more unstable angina in the paclitaxel group ($P = .02$). The mean number of lesions stented was 1.2 (SD, 0.4) in each group; 2 lesions were treated in 15.4% of patients in each group, whereas the remainder had 1 lesion treated. Lesion characteristics as measured by quantitative coronary angiography were also similar between the 2 groups (Table 1).

Procedural Results and Angiographic Outcomes

As shown in TABLE 2, the total stent length per lesion was slightly greater in the everolimus group, likely due to the fewer stent lengths available for accurate lesion matching. Conversely, implantation pressure was slightly less in the group receiving everolimus stents. Other procedural variables were well matched between the groups. Acute postprocedure angiographic measures were also not significantly different between the 2 groups.

Angiographic follow-up at 8 months was completed in 77% of eligible patients (Figure 1). The primary end point of in-segment late loss in the analysis lesion was significantly less in the everolimus group compared with the paclitaxel group (0.14 [SD, 0.41] mm [n=301 lesions] vs 0.28 [SD, 0.48] mm [n=134 lesions]; difference, −0.14 [95% CI, −0.23 to −0.05]; $P_{\text{noninferiority}} < .001$; $P_{\text{superiority}} = .004$). In-stent late loss in the analysis lesion was also significantly less in the everolimus group (0.16 [SD, 0.41] mm vs 0.31 [SD, 0.55] mm; difference, −0.15 [95% CI, −0.25 to −0.04]; $P_{\text{noninferiority}} < .001$; $P_{\text{superiority}} = .006$). Similar results were found when all lesions were considered (Table 2). As a result, strong trends were present toward a reduction in binary in-stent and in-segment restenosis with the everolimus stent compared with the paclitaxel stent (Table 2). No aneurysms were present at 8 months in either group.

Intravascular Ultrasound Findings

Volumetric intravascular ultrasound data were available at 8 months in 101

Table 2. Procedural Results and Angiographic Outcomes

Result/Outcome	Everolimus-Eluting Stent	Paclitaxel-Eluting Stent	*P* Value
Procedural variables, mean (SD)			
No. of patients	669	332	
No. of stents per patient	1.3 (0.6)	1.3 (0.5)	.27
No. of stents per lesion	1.2 (0.4)	1.1 (0.3)	.07
Maximum stent diameter per lesion, mm	3.0 (0.4)	3.0 (0.4)	>.99
Maximum stent to reference vessel diameter ratio	1.1 (0.1)	1.1 (0.1)	.56
Total stent length per lesion, mm	22.8 (8.4)	21.6 (7.8)	.02
Total stent to lesion length ratio	1.6 (0.5)	1.5 (0.5)	.01
Maximum pressure, atm	14.8 (2.9)	15.1 (2.6)	.049
Glycoprotein IIb/IIIa inhibitors used, No./total (%)	184/669 (27.5)	82/332 (24.7)	.36
Postprocedural angiographic results, mean (SD)			
No. of lesions	772	383	
Minimal luminal diameter, mm			
In-stent	2.71 (0.43)	2.74 (0.41)	.38
In-segment	2.37 (0.45)	2.36 (0.45)	.73
Diameter stenosis, %			
In-stent	0.3 (8.9)	−0.2 (9.9)	.37
In-segment	13.5 (7.6)	14.4 (7.1)	.06
Acute gain, mm			
In-stent	1.89 (0.48)	1.91 (0.47)	.56
In-segment	1.54 (0.51)	1.53 (0.50)	.62
8-mo angiographic follow-up, mean (SD)[a]			
No. of lesions	344	158	
Reference vessel diameter, mm	2.77 (0.43)	2.78 (0.42)	.84
Minimal luminal diameter, mm			
In-stent	2.56 (0.53)	2.45 (0.65)	.07
In-segment	2.22 (0.53)	2.12 (0.60)	.08
Diameter stenosis, %			
In-stent	5.9 (16.4)	10.3 (21.4)	.02
In-segment	18.8 (14.4)	22.8 (16.4)	.008
Late loss, mm			
In-stent	0.16 (0.41)	0.30 (0.53)	.002
In-segment	0.14 (0.39)	0.26 (0.46)	.003
Binary restenosis, No./total (%)			
In-stent	8/343 (2.3)	9/158 (5.7)	.06
In-segment	16/344 (4.7)	14/158 (8.9)	.07

[a] Analysis of all lesions.

lesions in the everolimus group and 41 in the paclitaxel group. The everolimus stent compared with the paclitaxel stent resulted in significantly less neointimal hyperplasia (10.13 [SD, 11.46] mm^3 vs 20.87 [SD, 31.51] mm^3, $P=.04$) and percent volume obstruction (6.9% [SD, 6.4%] vs 11.2% [SD, 9.9%], $P=.01$). Paired immediate postprocedure and follow-up intravascular ultrasound studies were available in 90 lesions in the everolimus group and 43 in the paclitaxel group. Comparing the everolimus and paclitaxel stents, there were no significant differences detected in the rates of incomplete stent apposition either at the completion of the procedure (34.4% vs 25.6%, respectively; $P=.33$) or at 8 months (25.6% vs 16.3%, $P=.27$). Late acquired incomplete stent apposition was infrequent in both groups (1.1% vs 2.3%, $P=.54$).

Clinical Outcomes

At 30 days there tended to be fewer myocardial infarctions among the patients randomized to receive the everolimus stent compared with the paclitaxel stent (7/667 patients [1.0%] vs 9/330 [2.7%], respectively; relative risk, 0.38 [95% CI, 0.14 to 1.02]; $P=.06$), with comparable rates of cardiac death (0% in both groups) and target lesion revascularization (3/667 patients [0.4%] vs 1/330 [0.3%], respectively; relative risk, 1.48 [95% CI, 0.15 to 14.21]; $P>.99$). At 9 months, everolimus stents compared with paclitaxel stents were noninferior for the major secondary end point of ischemia-driven target vessel failure (47/657 patients [7.2%] vs 29/321 [9.0%], respectively; difference, −1.9% [95% CI, −5.6% to 1.8%]; relative risk, 0.79 [95% CI, 0.51 to 1.23]; $P_{noninferiority}<.001$; $P_{superiority}=.31$). A nonsignificant trend was also present at 1 year for a 24% reduction in target vessel failure in patients randomized to receive everolimus stents rather than paclitaxel stents (56/653 patients [8.6%] vs 36/320 [11.3%], respectively; relative risk, 0.76 [95% CI, 0.51 to 1.13]; $P=.20$). Use of the everolimus stent compared with the paclitaxel stent resulted in significant reductions in the secondary end point of composite major adverse cardiac events, both at 9 months (30/657 patients [4.6%] vs 26/321 [8.1%]; relative risk, 0.56 [95% CI, 0.34 to 0.94]; $P=.03$) and at 1 year (39/653 patients [6.0%] vs 33/320 [10.3%]; relative risk, 0.58 [95% CI, 0.37 to 0.90]; $P=.02$).

As shown in TABLE 3, there were no significant differences between the everolimus stent and the paclitaxel stent in the 1-year rates of death (all cause, cardiac, or noncardiac) or of myocardial infarction (all, Q-wave, or non–Q-wave). Similarly, there were no significant differences between the 2 devices in the rates of stent thrombosis, either early (≤30 days) or late (>30 days), whether analyzed by the prespecified protocol definition or by post hoc Academic Research Consortium definitions. There were also no statistically significant differences in the rates of target lesion revascularization, target vessel revascularization, or target vessel failure between the 2 stents at 1 year. As shown in FIGURE 2, the difference between the hazard curves for major adverse cardiac events became apparent in the early postprocedural period due to fewer myocardial infarctions with the everolimus stent, and then spread further between 6 and 12 months due to fewer target lesion revascularization procedures with the everolimus stent. Of the 15 and 12 patients in the everolimus and paclitaxel groups who had a protocol-defined ischemic target lesion revascularization event by 1 year, 5 and 4 patients, respectively (33.3% in each group) underwent revascularization solely on the basis of a diameter stenosis greater than 70% demonstrated by quantitative coronary angiography. At 365 days, aspirin was being taken by 94.9% and 92.4%

Table 3. Clinical Outcomes at 1 Year

Outcome	No./Total (%)		P Value
	Everolimus-Eluting Stent (n = 655)	Paclitaxel-Eluting Stent (n = 321)	
Death	8/655 (1.2)	4/321 (1.2)	>.99
Cardiac	5/655 (0.8)	3/321 (0.9)	.72
Noncardiac	3/655 (0.5)	1/321 (0.3)	>.99
Myocardial infarction[a]	18/653 (2.8)	13/320 (4.1)	.33
Q-wave	2/653 (0.3)	1/320 (0.3)	>.99
Non–Q-wave	16/653 (2.5)	12/320 (3.8)	.31
Death or myocardial infarction	24/654 (3.7)	16/321 (5.0)	.39
Cardiac death or myocardial infarction[a]	22/653 (3.4)	15/320 (4.7)	.37
Stent thrombosis			
Protocol definition	5/647 (0.8)	2/317 (0.6)	>.99
≤30 d	3/667 (0.4)	0/330 (0)	.55
>30 d	2/646 (0.3)	2/317 (0.6)	.60
ARC			
Definite	5/652 (0.8)	0/319 (0)	.18
Probable	2/652 (0.3)	2/319 (0.6)	.60
Possible	4/652 (0.6)	2/319 (0.6)	>.99
Definite or probable	7/652 (1.1)	2/319 (0.6)	.73
Any	11/652 (1.7)	4/319 (1.3)	.78
Target lesion revascularization	22/655 (3.4)	18/321 (5.6)	.12
Target vessel revascularization	40/655 (6.1)	24/321 (7.5)	.41
Target vessel revascularization remote	20/655 (3.1)	14/321 (4.4)	.35
Major adverse cardiac events[a]	39/653 (6.0)	33/320 (10.3)	.02
Target vessel failure[a]	56/653 (8.6)	36/320 (11.3)	.20

Abbreviations: ARC, Academic Research Consortium.[14]
[a] Per the statistical analysis plan, since the composite target vessel failure and major adverse cardiac event end points included cardiac deaths only, patients with noncardiac deaths were excluded from the denominator.

of patients receiving everolimus stents and paclitaxel stents, respectively (P=.15), and a thienopyridine (clopidogrel or ticlopidine) was being taken by 71.2% and 70.4%, respectively (P=.82).

Subgroup Analysis

A post hoc linear regression analysis with formal interaction testing was performed to explore whether the reduction of the primary end point of in-segment late loss at 8 months with the everolimus stent compared with the paclitaxel stent was consistent across important subgroups (of which diabetes and the number of treated vessels were prespecified). As shown in FIGURE 3, there were no significant interactions between treatment assignment and angiographic outcomes among 7 subgroups, with the exception of age. Logistic regression analysis with interaction testing was also performed to explore whether the reduction in major adverse cardiac events with the everolimus stent compared with the paclitaxel stent present at 1 year was consistent across important subgroups. As shown in FIGURE 4, there were no significant interactions between treatment assignment and outcomes at 1 year among 8 subgroups, with the exception of patients with diabetes. The relative reduction in major adverse cardiac events with everolimus stents compared with paclitaxel stents was comparable in patients both undergoing and not undergoing 8-month follow-up angiography. Among patients in the angiographic follow-up cohort, target lesion revascularization in the everolimus and paclitaxel stent groups was required in 15 of 368 (4.1%) vs 12 of 181 (6.6%) patients, respectively (relative

Figure 2. Time-to-Event Curves for Cardiac Death or Myocardial Infarction, Target Lesion Revascularization, Major Adverse Cardiac Events, and Target Vessel Failure Among Patients Randomized to Receive the Everolimus-Eluting Stent and the Paclitaxel-Eluting Stent

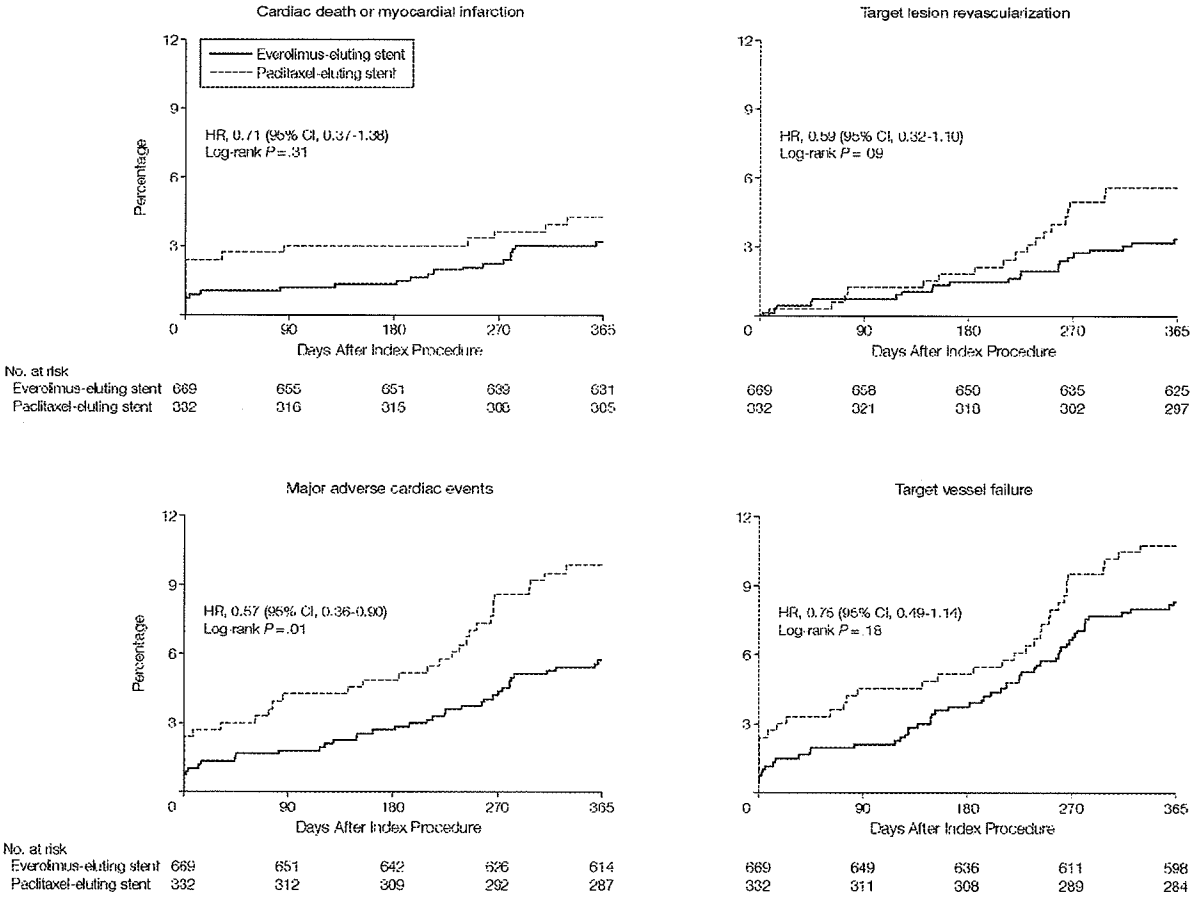

Event rates presented here were calculated by Kaplan-Meier methods and compared with the log-rank test and differ slightly from those in the text and Table 3, which were calculated as categorical variables and compared with the Fisher exact test. In each panel, initial number at risk for the paclitaxel stent differs from the number randomized because 1 patient did not sign informed consent. CI indicates confidence interval; HR, hazard ratio.

risk, 0.61 [95% CI, 0.29 to 1.29]; $P=.21$), whereas in the nonangiographic follow-up cohort the target lesion revascularization rates were 7 of 285 (2.5%) vs 6 of 139 (4.3%), respectively (relative risk, 0.57 [95% CI, 0.19 to 1.66]; $P=.37$).

COMMENT

This large-scale, prospective, randomized, single-blind, controlled study demonstrates that an everolimus-eluting stent compared with a widely used paclitaxel-eluting stent results in a significant reduction in angiographic in-segment late loss at 8 months, with noninferior 9-month rates of ischemia-driven target vessel failure. Thus, the 2 prespecified FDA regulatory requirements required for the trial to be considered successful were met. The reduction in late loss was confirmed by the findings from intravascular ultrasound, which demonstrated an approximate 50% reduction in volumetric neointimal hyperplasia. As a result, even though the trial was not powered for a reduction in binary angiographic restenosis, a strong trend was present in this direction favoring the everolimus-eluting stent.

Notably, the everolimus stent compared with the paclitaxel stent resulted in a significant 42% reduction in major adverse cardiac events at 1 year. As such, the present study is the first pivotal randomized trial to demonstrate enhanced event-free survival with a new stent compared with any of the 3 drug-eluting stents commercially available in the United States for on-label lesions (ie, those for which treatment with drug-eluting stents has been approved by the FDA). As defined in this trial, major adverse cardiac events is a composite measure of safety (cardiac death and myocardial infarction) and stent efficacy (target lesion revascularization), which is more specific to the action of the stent than is target vessel failure (which includes the occurrence of target vessel revascularization remote from the target lesion, which would not be expected to be affected by stent implantation). The reduction in composite major adverse cardiac events with the everolimus stent was attributable to fewer postprocedural non–Q-wave myocardial infarctions and late target lesion revascularizations due to the reduction in restenosis. In this regard the results of SPIRIT III confirm and extend those from the smaller (300 patients) randomized SPIRIT II trial, in which the 1-year rates of major adverse cardiac events (using the same definition) were decreased from 9.2% with a paclitaxel-eluting stent to 2.7% with an everolimus-eluting stent ($P=.04$), also due to fewer cardiac deaths, myocardial infarctions, and target lesion revascularizations.[19] Reduction in procedural-related myonecrosis with the everolimus stent may result from less side-branch compromise due to the thinner polymer (7.8 μm vs 16.0 μm) and total polymer plus stent strut width (89 vs 148 μm) compared with the paclitaxel stent,[20] though detailed angio-

Figure 3. Subgroup Analyses of the Primary End Point of 8-Month Angiographic In-Segment Late Loss Among Patients Randomized to Receive the Everolimus-Eluting Stent vs the Paclitaxel-Eluting Stent

	No. of randomized lesions		In-segment luminal late loss, mean (SD), mm			
	Everolimus-eluting stent	Paclitaxel-eluting stent	Everolimus-eluting stent	Paclitaxel-eluting stent	Difference (95% CI)	*P* for interaction
Angiographic follow-up cohort	343	168	0.14 (0.39)	0.26 (0.46)	−0.13 (−0.21 to 0.04)	
Age						
≥Median (63 y)	171	76	0.12 (0.37)	0.39 (0.55)	−0.27 (−0.41 to 0.14)	<.001
<Median	172	82	0.16 (0.42)	0.15 (0.33)	0.01 (−0.09 to 0.11)	
Sex						
Men	250	108	0.13 (0.34)	0.25 (0.49)	−0.12 (−0.23 to −0.02)	.94
Women	93	50	0.16 (0.51)	0.29 (0.41)	−0.13 (−0.28 to 0.03)	
Diabetes						
Yes	96	31	0.18 (0.51)	0.24 (0.40)	−0.06 (−0.23 to 0.12)	.34
No	247	127	0.12 (0.34)	0.27 (0.48)	−0.15 (−0.24 to −0.06)	
No. of treated vessels						
Single	258	110	0.13 (0.41)	0.30 (0.49)	−0.16 (−0.27 to −0.06)	.16
Dual	85	48	0.14 (0.33)	0.18 (0.39)	−0.04 (−0.17 to 0.09)	
Target vessel						
LAD	135	68	0.13 (0.40)	0.26 (0.49)	−0.13 (−0.27 to 0.00)	.92
Non-LAD	208	90	0.14 (0.39)	0.26 (0.45)	−0.12 (−0.23 to −0.02)	
RVD						
>Median (2.775 mm)	166	88	0.18 (0.38)	0.29 (0.54)	−0.11 (−0.24 to 0.02)	.74
≤Median	177	70	0.10 (0.41)	0.24 (0.36)	−0.14 (−0.24 to −0.03)	
Lesion length						
>Median (13.7 mm)	169	82	0.19 (0.47)	0.31 (0.51)	−0.12 (−0.25 to 0.01)	>.99
<Median	174	74	0.09 (0.30)	0.21 (0.40)	−0.12 (−0.22 to −0.02)	

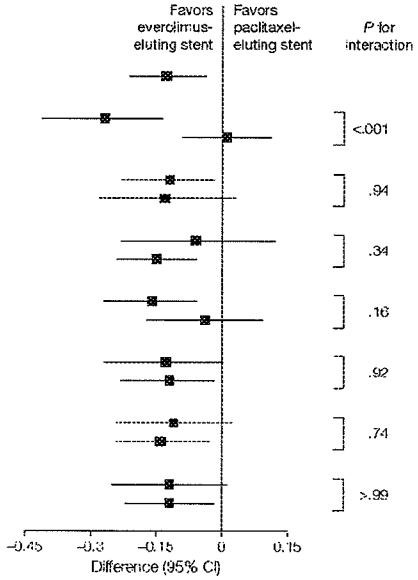

Probability for interaction represents the likelihood for interaction between the variable and the relative treatment effect. CI indicates confidence interval; LAD, left anterior descending; RVD, reference vessel diameter.

graphic study is required to confirm this possibility. Importantly, there were no significant differences in the occurrence of stent thrombosis through 1 year between these 2 devices, though this trial was underpowered to reliably evaluate this event; also, longer-term follow-up is required, because the incremental risk of stent thrombosis with drug-eluting stents may emerge beyond 1 year.[4] The lower rate of target lesion revascularization with the everolimus stent compared with the paclitaxel stent may be directly attributed to the reduction in late loss and smaller follow-up diameter stenosis in the target lesion, as recently described.[21]

The reduction in in-segment late loss with the everolimus stent compared with the paclitaxel stent was consistent across multiple important subgroups except when stratified by age. No significant differences in angiographic outcomes were present between the 2 stents in young patients, whereas assignment to receive the everolimus stent rather than the paclitaxel stent was associated with a marked reduction in late loss in elderly patients. Given the lack of an interaction with reference vessel diameter and lesion length, an explanation underlying this finding is not immediately evident. Of note, no interaction was present between diabetic status and angiographic late loss, signifying a significant reduction in in-segment late loss with the everolimus stent compared with the paclitaxel stent in patients both with and without diabetes. In contrast, a significant interaction was present between diabetes and stent type on the major adverse cardiac event end point, a finding that contributes to the conflicting reports from prior studies examining the relative safety and efficacy of paclitaxel-eluting compared with sirolimus-eluting stents in patients with diabetes.[22-25] However, this difference was driven by the 62% lower rate of major adverse cardiac events in patients with diabetes who were treated with paclitaxel stents compared with patients without diabetes who also were treated with paclitaxel stents, an unlikely finding that may have been due to chance alone. The differences between the 2 devices were also less apparent in larger vessels (which, compared with small vessels, may be able to accommodate more neointimal hyperplasia before the ischemic threshold is reached)[21] and in longer lesions (which, compared with shorter lesions, may have a greater statistical likelihood of restenosis developing in a

Figure 4. Subgroup Analyses of the 1-Year Rates of Major Adverse Cardiac Events Among Patients Randomized to Receive the Everolimus-Eluting Stent vs the Paclitaxel-Eluting Stent

	Major adverse cardiac events, No./total (%)				
	Everolimus-eluting stent	Paclitaxel-eluting stent	Relative Risk (95% CI)	Favors everolimus-eluting stent / Favors paclitaxel-eluting stent	*P* for interaction
Overall	39/653 (6.0)	33/320 (10.3)	0.56 (0.37 to 0.90)		
Age					
≥Median (63 y)	18/327 (5.5)	19/158 (12.0)	0.46 (0.25 to 0.85)		.28
<Median	21/326 (6.4)	14/162 (8.6)	0.75 (0.39 to 1.43)		
Sex					
Men	23/459 (5.0)	15/208 (7.2)	0.69 (0.37 to 1.30)		.46
Women	16/194 (8.2)	18/112 (16.1)	0.51 (0.27 to 0.97)		
Diabetes					
Yes	17/194 (8.8)	4/86 (4.7)	1.88 (0.65 to 5.43)		.01
No	22/459 (4.8)	29/232 (12.5)	0.38 (0.23 to 0.65)		
No. of treated vessels					
Single	31/552 (5.6)	22/270 (8.1)	0.69 (0.41 to 1.17)		.17
Dual	8/101 (7.9)	11/50 (22.0)	0.36 (0.15 to 0.84)		
Target vessels[a]					
LAD	15/232 (6.5)	12/119 (10.1)	0.64 (0.31 to 1.33)		.76
Non-LAD	16/320 (5.0)	10/150 (6.7)	0.75 (0.35 to 1.61)		
RVD[a]					
>Median (2.775 mm)	14/274 (5.1)	6/137 (4.4)	1.17 (0.46 to 2.97)		.14
≤Median	17/278 (6.1)	16/132 (12.1)	0.50 (0.26 to 0.97)		
Lesion length[a]					
>Median (13.7 mm)	21/271 (7.7)	11/138 (8.0)	0.97 (0.48 to 1.96)		.13
≤Median	10/281 (3.6)	11/129 (8.5)	0.42 (0.18 to 0.96)		
Follow-up cohort					
Angiographic	22/368 (6.0)	18/181 (9.9)	0.60 (0.33 to 1.09)		.85
Nonangiographic	17/285 (6.0)	15/139 (10.8)	0.55 (0.28 to 1.07)		

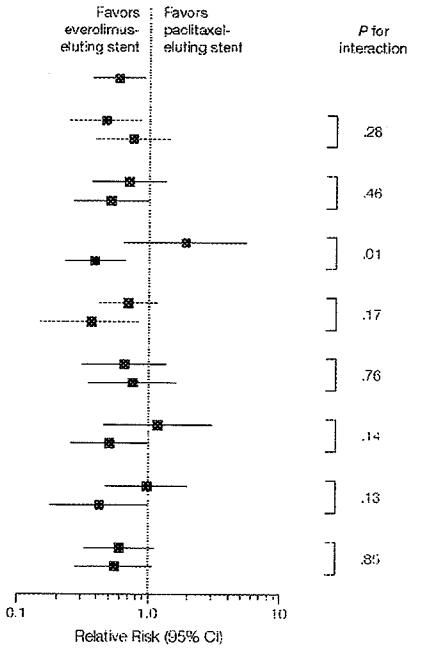

Probability for interaction represents the likelihood for interaction between the variable and the relative treatment effect. CI indicates confidence interval; LAD, left anterior descending; RVD, reference vessel diameter.
[a]Analysis restricted to patients undergoing treatment of a single lesion.

single spot, despite less volumetric neointimal hyperplasia). Moreover, no differences were evident in the beneficial effect of the everolimus stent compared with the paclitaxel stent in reducing the occurrence of major adverse cardiac events as a function of age. All of these subgroup findings should be considered hypothesis-generating, because subgroup analysis is inherently underpowered and statistical adjustments were not made for multiple comparisons leading to possible false-positive findings.[26]

The strengths and limitations of the present investigation should be considered. That composite major adverse cardiac events have now been shown to be reduced with an everolimus stent compared with a paclitaxel stent in 2 consecutive randomized trials performed at different institutions in different geographies (United States vs Europe and Asia Pacific)[19] increases the likelihood that this finding is real. Despite the dilutive effect of including target vessel revascularization in the target vessel failure end point, a trend was also present toward a 24% reduction with the everolimus stent in this composite measure at 1 year. Moreover, the clinical and angiographic outcomes with the paclitaxel stent in the present study were similar or better than those observed in earlier trials with this device in comparable patients and lesions,[2] and as such underperformance of the control stent does not explain this finding. However, while SPIRIT III is the largest completed trial to date investigating an everolimus-eluting stent, major adverse cardiac events were not the primary end point of this study (nor of SPIRIT II), and therefore this conclusion cannot be considered definitive until prospectively verified in an adequately powered randomized trial. The present trial also was underpowered to examine whether an everolimus stent reduces target lesion revascularization, target vessel revascularization, and target vessel failure as well as the occurrence of low-frequency safety events, compared with a paclitaxel stent. That angiographic follow-up was performed in 43.5% of patients in the present trial further raises concern whether the greater late loss with the paclitaxel stent compared with the everolimus stent may have triggered a greater proportion of excess revascularization procedures in the former group (the "oculostenotic reflex"),[27] although such a bias was not apparent in subgroup analysis. Logistic considerations precluded blinding the operator to the stent type, although clinical follow-up assessment, core laboratory, and clinical events committee personnel were blinded to randomization group, and source-documented ischemia or a severe stenosis by quantitative analysis was required to be present for declaration of target lesion or vessel revascularization. The results of the present trial cannot be extended to patient and lesion types excluded from enrollment. Also, complete screening log data are not available, and thus the proportion of patients undergoing percutaneous coronary intervention who were eligible for enrollment in this study is unknown. Finally, the current study was not designed to elicit other potential advantages of the everolimus stent, such as its greater flexibility and deliverability in complex coronary anatomy.

In summary, in this large-scale, prospective randomized trial, an everolimus-eluting stent compared with a paclitaxel-eluting stent in de novo native coronary artery lesions resulted in reduced angiographic late loss, noninferior rates of target vessel failure, and fewer major adverse cardiac events during 1 year of follow-up.

Author Affiliations: Columbia University Medical Center and The Cardiovascular Research Foundation, New York, New York (Drs Stone and Lansky); St Joseph Medical Center, Towson, Maryland (Dr Midei); Wake Medical Center, Raleigh, North Carolina (Dr Newman); St Patrick Hospital, Missoula, Montana (Dr Sanz); The Heart Center of Indiana, Indianapolis (Dr Hermiller); Presbyterian Hospital, Charlotte, North Carolina (Dr Williams); EMH Regional Medical Center, Elyria, Ohio (Dr Farhat); Duke Clinical Research Institute, Durham, North Carolina (Dr Mahaffey); Harvard Clinical Research Institute, Boston, Massachusetts (Dr Cutlip); Stanford University Medical Center, Stanford, California (Dr Fitzgerald), and Abbott Vascular, Santa Clara, California (Dr Sood and Ms Su).

Author Contributions: Dr Stone had full access to all of the data in the study and takes responsibility for the integrity of the data and the accuracy of the data analysis.

Study concept and design: Stone, Hermiller, Sood.
Acquisition of data: Midei, Newman, Sanz, Hermiller, Williams, Farhat, Mahaffey, Sood.
Analysis and interpretation of data: Stone, Williams, Cutlip, Fitzgerald, Su, Lansky.
Drafting of the manuscript: Stone, Sood.
Critical revision of the manuscript for important intellectual content: Midei, Newman, Sanz, Hermiller, Williams, Farhat, Mahaffey, Cutlip, Fitzgerald, Su, Lansky.
Statistical analysis: Su, Lansky.
Obtained funding: Hermiller.
Administrative, technical, or material support: Newman, Sanz, Hermiller, Williams, Cutlip, Sood.
Study supervision: Stone, Sanz, Farhat.

Financial Disclosures: Dr Stone reported receiving research support from Abbott Vascular and Boston Scientific Corp and honoraria from Medtronic. Dr Hermiller reported serving as a consultant for Abbott Vascular and Boston Scientific Corp. Dr Fitzgerald reported serving as a consultant for Abbott Vascular. Dr Mahaffey reported receiving research grants, consultancy fees, and speakers honoraria from Amgen, Bayer, Daiichi, Genentech, Johnson & Johnson, Lilly, Novartis, sanofi-aventis, sanofi-synthelabo, and Scios, and receiving research grants from Abbott Vascular, AstraZeneca, Bioheart, BMS, Boehringer Ingelheim, Boston Scientific, Cardiokinetix, Cierra, Conor, Cordis, Corgentech, Edwards, GE Medical Systems, Innocoll, KCI, Medtronic, Momenta, Portola, Sicel Technologies, and The Medicines Company. No other disclosures were reported.

Funding/Support: This study was sponsored and funded by Abbott Vascular, Santa Clara, California. Abbott supplied the everolimus-eluting stents; the paclitaxel-eluting stents were commercially purchased.

Role of the Sponsor: Abbott Vascular was involved in the design and conduct of the study; the collection, management, initial analysis, and interpretation of the data; and had the right to a nonbinding review of the manuscript. Approval of the sponsor was not required prior to submission.

Independent Statistical Analysis: The accuracy of the data analysis was independently verified by Martin Fahy, MSc, from the Cardiovascular Research Foundation (CRF), an affiliate of Columbia University College of Physicians and Surgeons. (The dean of Columbia University is responsible for this collaboration with the CRF and empowers an active oversight committee to monitor this relationship and the activities of the CRF.) Mr Fahy received the entire raw database and replicated all of the analyses that were reported in the manuscript, and no discrepancies were discovered. The results reported in this article are the results based on this independent analysis. Neither Mr Fahy nor the CRF received any funding for this independent analysis.

SPIRIT III Trial Organization and Participating Investigators: Steering Committee: G. W. Stone (Principal Investigator) and A. J. Lansky, Columbia University Medical Center and the Cardiovascular Research Foundation, New York, New York; G. Johnson, K. Sudhir, G. Thompson, T. Engels, R. White, J. Coe, C. Lewis, and J. Doostzadeh, Abbott Vascular, Santa Clara, California. Past member: C. Rogers (involved with protocol development and early trial initiation), formerly Brigham and Women's Hospital, Boston, Massachusetts, currently with Cordis Corp, Miami Lakes, Florida. **Data Monitoring:** Abbott Vascular, Santa Clara, California; Paragon Biomedical, Irvine, California. **Data Management and Biostatistical Analysis:** Abbott Vascular, Santa Clara, California. **Clinical Events Adjudication Committees:** *Duke Clinical Research Institute, Durham, North Carolina (primary protocol-specified events):* K. Mahaffey (Director), J. Petersen (lead physician), M. Meyer (lead coordinator), R. Mehta, A. Goyal, T. Wang, D. Montgomery, A. Wright, P. Connolly, R. Doletski; *Harvard Clinical Research In-*

stitute, Boston, Massachusetts (stent thrombosis adjudication per Academic Research Consortium definitions): D. Cutlip (Director), C. Berger, L Epstein, S. Waxman, J. Markis. **Data and Safety Monitoring Board:** Axio Research Company, Seattle, Washington; *Brigham and Women's Hospital, Boston, Massachusetts*: D. Faxon (Chair); *Clinimetrics Clinical Research Associates, San Jose, California*: L. Pennelly; *University of Kentucky, Lexington*: D. Moliterno; *University of Florida, Jacksonville*: M. Costa; *Campbell Heart Institute, Nashville, Tennessee*: R. Piana. **Angiographic Core Laboratory:** *Cardiovascular Research Foundation, New York, New York*: A. J. Lansky (Director), E. Cristea. **Intravascular Ultrasound Imaging Core Laboratory:** *Stanford Center for Research in Cardiovascular Intervention, Palo Alto, California*: P. Fitzgerald (Director). **Study Sites, Principal Investigators, and Primary Study Coordinators:** *Baptist Medical Center Princeton, Birmingham, Alabama* (A. Bouchard, W. Wade); *Trinity Medical Center, Birmingham, Alabama* (J. Eagan, B. Williams); *Arizona Heart Hospital, Phoenix* (R. Strumpf, L. Grow); *Scripps Memorial Hospital, La Jolla, California* (R. Fortuna, S. Weaver); *Good Samaritan Hospital, Los Angeles, California* (R. Matthews, S. Mullin); *Alta Bates Summit Medical Center, Oakland, California* (R. Feldman, J. Ingram), *Mercy General Hospital, Sacramento, California* (M. Chang, S. Bordash); *Poudre Valley Hospital, Fort Collins, Colorado* (A. Doing, D. Robeson); *Washington Hospital Center, Washington, DC* (L. Satler, S. Pokharel); *North Ridge Medical Center, Ft Lauderdale, Florida* (A. Niederman, T. Kellerman); *Baptist Hospital of Miami, Miami, Florida* (R. Quesada, C. Hodgson); *Emory Crawford Long Hospital, Atlanta, Georgia* (H.A. Liberman, T. Sanders); *Piedmont Hospital, Atlanta, Georgia* (C. Brown, N. Flockhart); *Saint Joseph's Hospital of Atlanta, Atlanta, Georgia* (M. Unterman, W. Knapp, P. Patel); *Rush University Medical Center, Chicago, Illinios* (G. Schaer, K. Abdul-Ahad); *Elmhurst Memorial Hospital, Lombard, Illinois* (M. Brottman, L. Elder); *St John's Hospital, Springfield, Illinois* (G. Mishkel, P. Warren); *The Heart Center of Indiana LLC, Indianapolis* (J. Hermiller, S. Gallagher), *Jewish Hospital, Louisville, Kentucky* (N. Xenopoulos, B. Henehan); *Ochsner Clinic Foundation, New Orleans, Lousiana* (S. Ramee, B. Hirstius), *Brigham and Women's Hospital, Boston, Massachusetts* (L. Mauri, D. Manuelian); *Johns Hopkins Hospital, Baltimore, Maryland* (J. Resar, K. Citro); Barnes-Jewish Hospital, St Louis, Missouri (J. Lasala, K. Striler); *Washington Adventist Hospital, Takoma Park, Maryland* (M. Turco, D. Shaddinger); *St Joseph Medical Center, Towson, Maryland* (M. Midei, E. Yaker); *St John Hospital and Medical Center, Detroit, Michigan* (T. Davis, M. O'Bryan); *Spectrum Health Hospital, Grand Rapids, Michigan* (D. Wohns, H. Singh, K. Postema); *Borgess Medical Center, Kalamazoo, Michigan* (T. Fischell, J. Stauffer); *Northern Michigan Hospital, Petoskey* (L. Cannon, J. LaLonde); *Abbott Northwestern Hospital, Minneapolis, Minnesota* (M. Mooney, C. Stone); *St Luke's Hospital, Kansas City, Missouri* (A. Grantham, C. Rutherford); *North Mississippi Medical Center, Tupelo* (B. Bertolet, K. Glenn); *St Patrick Hospital, Missoula, Montana* (M. Sanz, H. Boehm); *Presbyterian Hospital, Charlotte, North Carolina* (J. Williams, A. Maganares); *Duke University Medical Center, Durham, North Carolina* (J. Zidar, D. Glisson); *Wake Medical Center, Raleigh, North Carolina* (W. Newman, S. Darden); *Wake Forest University Health Sciences, Winston-Salem, North Carolina* (R. Applegate, T. Young); *Nebraska Heart Hospital, Lincoln* (D. Netz, R. Holcomb); *Dartmouth-Hitchcock Medical Center, Lebanon, New Hampshire* (A.V. Kaplan, L. Martel); *Hackensack Medical Center, Hackensack, New Jersey* (V. Sethi, M. Reid); *The Valley Hospital, Ridgewood, New Jersey* (C. Hirsch, K. Sayles); *Presbyterian Hospital, Albuquerque, New Mexico* (N. Shadoff, P. Nail); *St Joseph's Hospital Health Center, Liverpool, New York* (R. Caputo, C. Lastinger); *Long Island Jewish Medical Center, New Hyde Park, New York* (B. Kaplan, B. Gonzales); *Columbia University Medical Center, New York, New York* (M. Collins, V. Laroche); *The Christ Hospital, Cincinnati, Ohio* (D. Kereiakes, D. White); *Riverside Methodist Hospital, Columbus, Ohio* (S. Yakubov, T. Edwards); *EMH Regional Medical Center, Elyria, Ohio* (N. Farhat, A. Giunta); *Integris Baptist Medical Center Inc, Oklahoma City, Oklahoma* (S. Prabhu, B. Pentrina); *University of Oklahoma Health Sciences Center, Oklahoma City* (J. Saucedo, D. Beard); *Sacred Heart Medical Center, Eugene, Oregon* (J. Chambers, D. Butler); *Providence St Vincent Medical Center, Portland, Oregon* (T. Caulfield, E. Johnson); *Allegheny General Hospital, Pittsburgh, Pennsylvania* (T. Farah, C. Harter); *Pinnacle Health at Harrisburg Hospital, Wormleysburg, Pennsylvania* (W. Bachinsky, A. Todd); *Rhode Island Hospital, Providence* (D. Williams, J. Muratori); *The Miriam Hospital, Providence, Rhode Island* (P. Gordon, L. DeSimone); *Medical University of South Carolina, Charleston* (C. Nielsen, B. Owens); *Heart Hospital of Austin, Austin, Texas* (R. Gammon, M. Robison); *Medical City Dallas Hospital, Dallas, Texas* (D. Brown, T. Goldston); *The Methodist Hospital, Houston, Texas* (N. Kleiman, H. Campbell); *TexSan Heart Hospital, San Antonio, Texas* (W. Wu, G. Carreon); *Fletcher Allen Health Care, Burlington, Vermont* (H. Dauerman, F. Straight); *Swedish Medical Center, Seattle, Washington* (M. Reisman, J. Hudacheck); *St Luke's Medical Center, Milwaukee, Wisconsin* (P. Berstein, S. Oxborough).

REFERENCES

1. Al Suwaidi J, Berger PB, Holmes DR. Coronary artery stents. *JAMA*. 2000;284(14):1828-1836.
2. Stone GW, Ellis SG, Cox DA, et al. A polymer-based paclitaxel-eluting stent in patients with coronary artery disease. *N Engl J Med*. 2004;350(3):221-231.
3. Moses JW, Leon MB, Popma JJ, et al. Sirolimus-eluting stents versus standard stents in patients with stenosis in a native coronary artery. *N Engl J Med*. 2003;349(14):1315-1323.
4. Stone GW, Moses JW, Ellis SG, et al. Safety and efficacy of sirolimus- and paclitaxel-eluting coronary stents. *N Engl J Med*. 2007;356(10):998-1008.
5. Daemen J, Wenaweser P, Tsuchida K, et al. Early and late coronary stent thrombosis of sirolimus-eluting and paclitaxel-eluting stents in routine clinical practice. *Lancet*. 2007;369(9562):667-678.
6. Finn AV, Joner M, Nakazawa G, et al. Pathological correlates of late drug-eluting stent thrombosis. *Circulation*. 2007;115(18):2435-2441.
7. Kotani J, Awata M, Nanto S, et al. Incomplete neointimal coverage of sirolimus-eluting stents. *J Am Coll Cardiol*. 2006;47(10):2108-2111.
8. Marx SO, Marks AR. Bench to bedside: the development of rapamycin and its application to stent restenosis. *Circulation*. 2001;104(8):852-855.
9. Eisen HJ, Tuzcu EM, Dorent R, et al. Everolimus for the prevention of allograft rejection and vasculopathy in cardiac-transplant recipients. *N Engl J Med*. 2003;349(9):847-858.
10. Avery RK. Cardiac-allograft vasculopathy. *N Engl J Med*. 2003;349(9):829-830.
11. Joner M, Quee SC, Coleman L, et al. Competitive comparison of reendothelialization in drug eluting stents. *Circulation*. 2006;114(suppl II):II-506.
12. Serruys PW, Ong ATL, Piej JJ, et al. A randomised comparison of a durable polymer everolimus-eluting coronary stent with a bare metal coronary stent. *EuroIntervention*. 2005;1:58-65.
13. Serruys PW, Ruygrok P, Neuzner J, et al. A randomised comparison of an everolimus-eluting coronary stent with a paclitaxel-eluting coronary stent: the SPIRIT II trial. *EuroIntervention*. 2006;2:286-294.
14. Cutlip DE, Windecker S, Mehran R, et al. Clinical endpoints in coronary stent trials—a case for standardized definitions. *Circulation*. 2007;115(17):2344-2351.
15. Lansky AJ, Dangas G, Mehran R, et al. Quantitative angiographic methods for appropriate endpoint analysis, edge-effect evaluation, and prediction of recurrent restenosis after coronary brachytherapy with gamma irradiation. *J Am Coll Cardiol*. 2002;39(2):274-280.
16. Mintz GS, Nissen SE, Anderson WD, et al. American College of Cardiology Clinical Expert Consensus Document on Standards for Acquisition, Measurement and Reporting of Intravascular Ultrasound Studies (IVUS): a report of the American College of Cardiology Task Force on Clinical Expert Consensus Documents. *J Am Coll Cardiol*. 2001;37(5):1478-1492.
17. Kastrati A, Schömig A, Elezi S, et al. Interlesion dependence of the risk for restenosis in patients with coronary stent placement in multiple lesions. *Circulation*. 1998;97(24):2396-2401.
18. Morikawa T, Yoshida M. A useful testing strategy in phase III trials: combined test of superiority and test of equivalence. *J Biopharm Stat*. 1995;5(3):297-306.
19. Ruygrok P. SPIRIT II study: a clinical evaluation of the XIENCE V everolimus eluting coronary stent system in the treatment of patients with de novo native coronary artery lesions. *J Am Coll Cardiol*. 2007;49(suppl B):28B.
20. Stone GW, Ellis SG, Cannon L, et al; TAXUS V Investigators. Comparison of a polymer-based paclitaxel-eluting stent with a bare metal stent in patients with complex coronary artery disease: a randomized controlled trial. *JAMA*. 2005;294(10):1215-1223.
21. Pocock SJ, Lansky AJ, Mehran R, et al. Angiographic surrogate endpoints in drug-eluting stent trials. *J Am Coll Cardiol*. 2008;51(1):23-32.
22. Morice MC, Colombo A, Meier B, et al. Sirolimus- vs paclitaxel-eluting stents in de novo coronary artery lesions. *JAMA*. 2006;295(8):895-904.
23. Windecker S, Remondino A, Eberli FR, et al. Sirolimus-eluting and paclitaxel-eluting stents for coronary revascularization. *N Engl J Med*. 2005;353(7):653-662.
24. Dibra A, Kastrati A, Mehilli J, et al. Paclitaxel-eluting or sirolimus-eluting stents to prevent restenosis in diabetic patients. *N Engl J Med*. 2005;353(7):663-670.
25. Spaulding C, Daemen J, Boersma E, Cutlip DE, Serruys PW. A pooled analysis of data comparing sirolimus-eluting stents with bare-metal stents. *N Engl J Med*. 2007;356(10):989-997.
26. Hernández AV, Boersma E, Murray GD, Habbema JD, Steyerberg EW. Subgroup analyses in therapeutic cardiovascular clinical trials: are most of them misleading? *Am Heart J*. 2006;151(2):257-264.
27. Serruys PW, van Hout B, Bonnier H, et al. Randomised comparison of implantation of heparin-coated stents with balloon angioplasty in selected patients with coronary artery disease (Benestent II). *Lancet*. 1998;352(9129):673-681.

ELSEVIER

Journal of Chromatography B, 718 (1998) 251–257

JOURNAL OF CHROMATOGRAPHY B

Quantitative analysis of sirolimus (Rapamycin) in blood by high-performance liquid chromatography–electrospray tandem mass spectrometry

Paul J. Taylor*, Anthony G. Johnson

Centre for Clinical and Experimental Therapeutics, University of Queensland, Department of Medicine, Princess Alexandra Hospital, First Floor Lions Clinical Research Building, Ipswich Road, Brisbane, Queensland 4102, Australia

Received 5 May 1998; received in revised form 28 July 1998; accepted 28 July 1998

Abstract

We report here a quantitative method for the analysis of sirolimus in blood using solid-phase sample preparation and HPLC–electrospray-tandem mass spectrometry detection. Blood samples (500 • l) were prepared by pre-treatment with acetonitrile: 15 m*M* zinc sulphate (70:30, v/v), containing 32-demethoxysirolimus (internal standard) and C_{18} solid-phase extraction. The electrospray conditions were chosen to enhance the $[M• NH_4]^+$ species at the expense of other species. Detection was by multiple reactant monitoring with the mass transitions *m/z* 931.8→864.6 and *m/z* 901.8→834.4 employed for sirolimus and the internal standard, respectively. The method was linear over the range 0.2 to 100.0 • g l^{-1}. The accuracy and inter-day precision, over this concentration range, was 94.4% to 104.4% and 1.4% to 5.0%, respectively. The accuracy and total precision at the limit of quantitation (0.2 • g l^{-1}) was 103.0% and 10.8%, respectively. The mean absolute recovery of sirolimus and the internal standard were 80.5% and 81.3%, respectively. The sensitivity and analytical concentration range of the method make it suitable for therapeutic drug monitoring and pharmacokinetic studies. Further, the ability of the method to measure parent drug specifically will facilitate the evaluation of immunoassays for sirolimus.

Keywords: Sirolimus; Rapamycin

1. Introduction

Sirolimus (Rapamycin, Rapamune®) is a macrolide lactone (Fig. 1), structurally related to tacrolimus, produced from the fermentation of *Streptomyces hygroscopicus* [1,2]. Sirolimus has a novel mechanism of action in that it inhibits the transduction of cytokine signals necessary for the proliferation and maturation of T cells at a later stage than tacrolimus or cyclosporine [3]. In vitro studies have shown sirolimus to be of similar potency to tacrolimus and up to 100 times more potent than cyclosporine, in terms of immunosuppressive activity [4]. Further, sirolimus has been shown to display a synergistic interaction with cyclosporine for both in vitro proliferation and cytotoxicity assays with rat or human lymphocytes and in vivo in rat, mouse and canine allograft models [5,6]. Phase II and III studies are under way evaluating sirolimus in combination

*Corresponding author.

0378-4347/98/$ – see front matter
PII: S0378-4347(98)00371-5

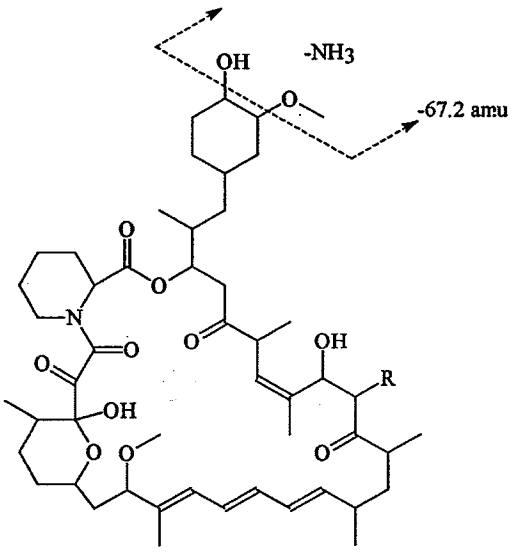

Fig. 1. Structures of sirolimus (R• O-CH_3) and the internal standard (R• H). The collision induced fragmentation (• 67.2 amu) of the analytes, used for selected reaction monitoring, is shown by the dotted line.

with cyclosporine in various solid organ transplant recipients.

The blood measurement of sirolimus is important in determining the dosage regimen, drug exposure, and a therapeutic range and in evaluating potential drug interactions. Further, therapeutic drug monitoring of other immunosuppressive drugs (eg. cyclosporine, tacrolimus) has been required due to the risk of rejection at low drug concentrations and toxicity and infection at high concentrations. In animal studies, a relationship between trough sirolimus concentration and both immunosuppressive efficacy and toxicity has been reported [7]. The pharmacokinetics of sirolimus in renal transplant recipients have been shown to vary widely between patients [8–10]. Zimmerman and Kahan reported a 4.5-fold variability in clearance, steady-state volume of distribution and blood/plasma ratio [10]. The metabolism of sirolimus is primarily by the cytochrome P450III A isozyme [11]. Thus sirolimus is susceptible to a number of potential drug interactions as a wide variety of inducers and inhibitors of this isozyme have been reported [12]. All of these factors make accurate and precise measurement of sirolimus vital for the optimal usage of the drug.

From the consensus report on sirolimus at the 1995 Lake Louise Consensus Conference on Immunosuppressant Drugs [13], a recommendation was made that whole blood should be the sample matrix of choice for measurement until one matrix is shown to be more clinically important as sirolimus is approximately 95% sequestered within the erythrocytes [14]. Although the concentration of sirolimus is much higher in whole blood than plasma, the quantification of sirolimus in blood is difficult because the circulating concentrations are generally below 100 • $g l^{-1}$. Sirolimus has a maximum absorptivity at 288, 277 and 267 nm, due to its triene structure [2] thus enabling high-performance liquid chromatography (HPLC)–UV analysis at such concentrations. Although a limit of quantification between 1.0 and 5.0 • $g l^{-1}$ has been reported with these methods, either complex sample extraction procedures or lengthy chromatographic analysis time (• 20 min) are significant limitations [15–18]. Streit et al. reported a HPLC–mass spectrometry method for the quantification of sirolimus and the detection of four sirolimus metabolites [19]. This method utilized an electrospray interface with single ion monitoring detection.

In this paper, we report a validated HPLC–electrospray tandem mass spectrometry (HPLC–ESI-MS–MS) method to quantitate sirolimus in whole blood using a solid-phase sample preparation.

2. Materials and methods

2.1. Chemicals and reagents

HPLC grade acetonitrile and methanol were purchased from EM Science (Gibbstown, NJ, USA). Reagent grade deionised water was obtained from a Milli-Q water purification system (Millipore, Milford, MA, USA). Sirolimus and the sirolimus analogue, 32-O-desmethoxysirolimus (internal standard) were a gift from Wyeth–Ayerst Research (Princeton, NJ, USA). Sirolimus and internal standard stock solutions were prepared in methanol and stored at • 75•C. A precipitation reagent, consisting of acetonitrile and 0.1 *M* zinc sulphate (70:30, v/v), was prepared containing internal standard (50 • $g l^{-1}$). All other chemicals were AR grade.

2.2. HPLC–mass spectrometric apparatus and conditions

The HPLC system consisted of a 616 pump with a 600S controller, a column oven with temperature control module (Waters, Milford, MA, USA) and an IS200 autosampler (Perkin Elmer, Danbury, CT, USA). The HPLC column was an Novapak C18 column (150 mm• 2.1 mm I.D., 4 • m, Waters), maintained at a temperature of 50•C. The mobile phase consisted of 80% methanol and 20% 50 m*M* ammonium acetate buffer (pH 5.1). The system operated at a flow-rate of 0.2 ml/min with approximately 1/10 of the flow split post-column into the mass spectrometer.

Mass spectrometric detection was performed on an API III triple quadrupole instrument (PE-Sciex, Thornhill, Toronto, Canada) using selected reaction monitoring. An electrospray interface was used in positive ionisation mode. The orifice potential was set at 55 V to produce predominantly ammoniated species of the analytes. The interface heater was set at 60•C. For collision-activated dissociation, argon was used as the collision gas at a thickness of 300• 10^{12} molecules $cm^{\bullet 2}$. Peak area ratios obtained from selected reaction monitoring of the mass transitions for sirolimus (*m/z* 931.8→864.6) and the internal standard (*m/z* 901.8→834.4) were used for quantification. Standard curves (0.2, 0.4, 1.0, 5.0, 10.0, 25.0, 80.0 and 100.0 • $g\,l^{\bullet -1}$) were constructed using weighted ($1/x^2$) linear least-squares regression. Data were collected and analysed on a Macintosh computer operating RAD and MACQUAN software (PE-Sciex).

2.3. Sample preparation

Standards, controls and patient samples (500 • l) were treated with precipitation reagent (2 ml) in 12-ml glass culture tubes. Samples were vortex-mixed and centrifuged (5 min, 850 *g*). The supernatants were applied to C18 solid-phase extraction cartridges (Isolute, 200 mg, 3 ml, Activon Scientific, Brisbane, QLD, Australia) which had been preconditioned with methanol (6 ml) and water (6 ml). The loaded cartridges were washed sequentially with water (6 ml), 50% methanol-water (3 ml) and heptane (2 ml). The washed cartridges were placed under full vacuum for 15 min. The analytes were eluted with 50% isopropyl alcohol-heptane (1 ml) and the eluents evaporated under air flow (45•C). Samples were dissolved in mobile phase (50 • l) and a 10 • l aliquot was injected.

2.4. Assay validation studies

Specificity of the assay was tested by analysing a total of 20 blood samples from different transplant recipients not receiving sirolimus therapy. Linearity was tested by analysing whole blood standards, prepared fresh on each day, containing known (weighed-in) amounts of sirolimus over a concentration range (0.2 to 100.0 • $g\,l^{\bullet -1}$, *n*• 6). A weighted linear regression model ($1/x^2$) was used throughout the study to adjust for differential variability across the wide concentration range used. The accuracy and inter-day precision were determined from the back-calculated results of the linearity study (*n*• 6). The precision and accuracy of the method was determined by assaying spiked whole blood controls (0.2, 0.5, 20.0 and 50.0 • $g\,l^{\bullet -1}$) in batches of five on each of four days. Intra-day, inter-day and total precision were derived from analyses of variance of the assayed controls using the method of Krouwer and Rabinowitz [20]. Accuracy was determined by expressing the mean assayed result for the control samples (*n*• 12) as a percentage of the weighed-in concentration. Absolute recoveries of the analytes were determined by comparing the peak areas of extracted samples, from ten different subjects, spiked with sirolimus and internal standard before and after extraction. The relative recovery of sirolimus was calculated from the ratio of sirolimus and internal standard absolute recoveries, expressed as a percentage (*n*• 10).

3. Results

Under the HPLC–ESI-MS–MS operating conditions, the predominant precursor ions for sirolimus and the internal standard were the ammoniated ion $[M\bullet\ NH_4]^{\bullet}$, *m/z* 931.8 and *m/z* 901.8, respectively. Collision-induced fragmentation of these precursor ions gave the predominant product ions (• 67.2 amu)

for sirolimus and the internal standard of *m/z* 864.6 and *m/z* 834.4, respectively (Fig. 1). These mass transitions, *m/z* 931.8→864.6 and *m/z* 901.8→834.4, were utilised for selected reaction monitoring.

The chromatographic conditions utilised in this method achieved retention times of 7.8 min for sirolimus and 8.4 min for the internal standard, thus giving a total chromatographic run time of 10 min. The specificity of the HPLC–ESI-MS–MS assay is illustrated in Fig. 2 by the chromatograms of (A) sirolimus-free blood, (B) sirolimus-free blood spiked with internal standard and (C) sirolimus-free blood spiked with sirolimus. These chromatograms show no interferences at the retention times of the analytes. Further, a total of 20 blood samples analysed, from different transplant recipients not receiving sirolimus therapy, showed no interference at the retention times of the analytes. Typical chromatograms of (A) a sirolimus blood standard (0.2 • g l^{-1}), (B) a sirolimus blood standard (100.0 • g l^{-1}) and (C) a blood sample obtained from a renal transplant recipient receiving 5 mg/day of sirolimus orally (3.7 • g l^{-1}) are illustrated in Fig. 3.

The HPLC–ESI-MS–MS assay was linear over the range 0.2 to 100.0 • g l^{-1} (r• 0.997, n• 6, Table

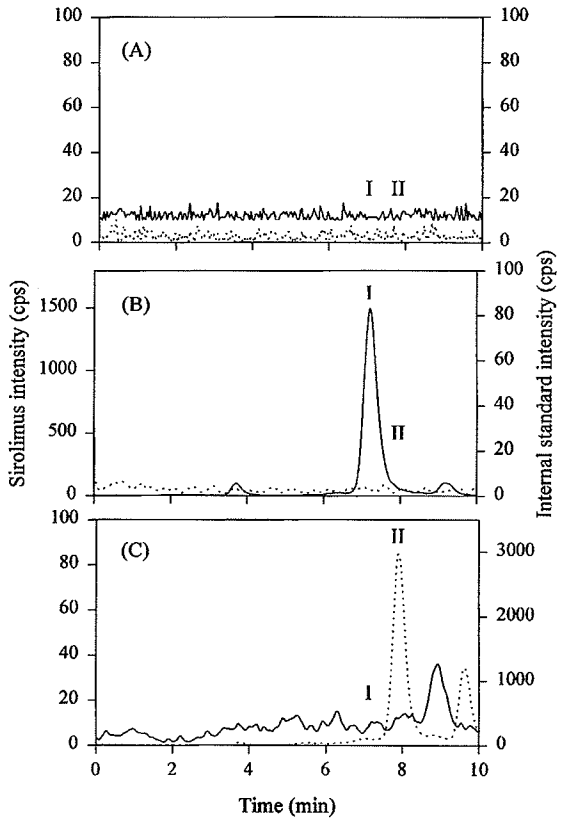

Fig. 2. The specificity of the method is illustrated with chromatograms of (A) sirolimus-free blood, (B) sirolimus-free blood spiked with sirolimus (10.0 • g l^{-1}) and (C) sirolimus-free blood spiked with internal standard (50.0 • g l^{-1}). The solid line represents sirolimus (*m/z* 931.8→864.6) and the dotted line represents the internal standard (*m/z* 901.8→834.4). The retention time of sirolimus and the internal standard are shown by I and II, respectively.

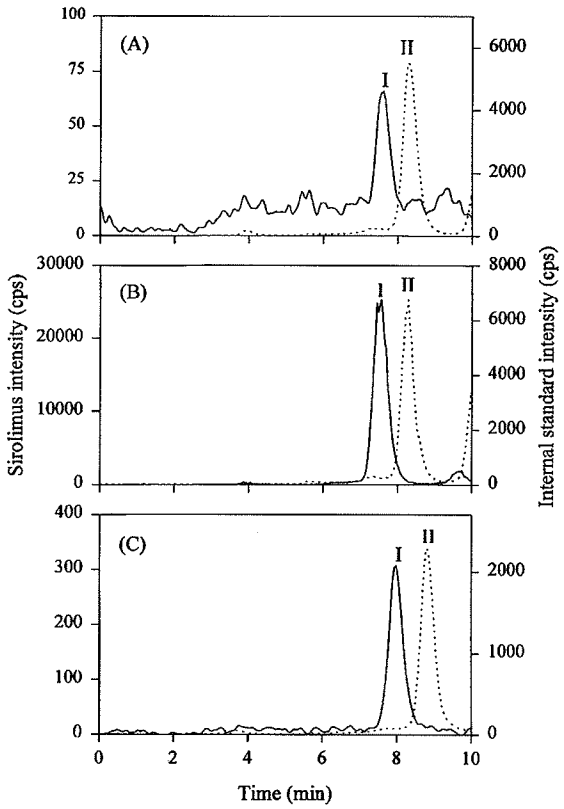

Fig. 3. Typical chromatograms of (A) a sirolimus blood standard (0.2 • g l^{-1}), (B) a sirolimus blood standard (100.0 • g l^{-1}) and (C) a blood sample obtained from a renal transplant recipient receiving 5 mg/day of sirolimus orally (3.7 • g l^{-1}). The internal standard concentration for all samples is 50.0 • g l^{-1}. The solid line represents sirolimus (*m/z* 931.8→864.6) and the dotted line represents the internal standard (*m/z* 901.8→834.4). The retention time of sirolimus and the internal standard are shown by I and II, respectively.

Table 1
Linearity[a], accuracy[b] and inter-day precision[c] of the HPLC–ESI–MS/MS assay, over the analytical range (0.2–100.0 • g l^{-1})

Day	$S_{y.x}$	Slope (S.E.)[d]	Intercept (S.E.)	Sirolimus concentration (• g l^{-1})							
				0.2	0.4	1.0	5.0	10.0	25.0	80.0	100
1	0.855	0.958 (0.008)	0.469 (0.377)	0.205	0.378	0.995	5.31	10.1	25.9	77.9	95.3
2	0.775	0.922 (0.007)	0.608 (0.342)	0.195	0.411	1.03	5.27	10.5	25.1	74.0	92.7
3	1.58	0.970 (0.015)	0.093 (0.695)	0.198	0.402	1.03	5.53	9.43	25.1	74.7	99.3
4	1.00	0.966 (0.010)	0.501 (0.442)	0.210	0.369	0.924	5.23	10.8	25.7	79.1	95.7
5	1.05	0.975 (0.010)	0.264 (0.462)	0.203	0.390	0.990	4.95	10.5	25.8	76.4	98.9
6	2.12	0.955 (0.020)	0.318 (0.937)	0.198	0.405	1.00	5.04	10.8	25.4	72.7	98.7
Mean Concentration (• g l^{-1})				0.202	0.393	0.995	5.22	10.4	25.5	75.8	96.8
accuracy (%)				100.8	98.1	99.5	104.4	104.0	102.0	94.8	96.8
Inter-day Precision (%)				2.7	4.2	3.9	3.9	5.0	1.4	3.2	2.7

[a] Linearity• standard error of the estimate ($S_{y.x}$).
[b] Accuracy• mean sirolimus concentration over weighed-in sirolimus concentration• 100%.
[c] Inter-day precision• coefficient of variation.
[d] (S.E.)• standard error.

1). The method's accuracy and inter-day precision, over the linear range, was 94.8% to 104.4% and 1.4% to 5.0%, respectively (Table 1). We defined the lower limit of quantitation of the method to be 0.2 • g l^{-1}. The performance of the method at this concentration was acceptable under the guidelines defined by Shah et al. [21]. The accuracy of the method at four control concentrations (0.2, 0.5, 20.0 and 50.0 • g l^{-1}) ranged from 95.2% to 103.0% (Table 2). The precision of the method, expressed in terms of intra-day, inter-day and total coefficients of variation, was • 11.0% over the range of control concentrations studied (Table 2). To extend the analytical range, a control was prepared at 200 • g l^{-1} diluted with blank blood 100:400 • l and assayed in replicate (n• 5). The dilution study achieved acceptable accuracy and intra-day precision of 97.1% and 4.0%, respectively. The mean absolute recovery (n• 10) of sirolimus and the internal standard were determined to be 80.5% and 81.3%, respectively, whilst the relative recovery of sirolimus to the internal standard was 99.4% (n• 10).

4. Discussion and conclusions

The neutral nature of sirolimus required the addition of ammonium acetate to the mobile phase in

Table 2
Precision[a] and accuracy[b] of HPLC–ESI–MS/MS assay determined for weighed-in controls (n• 20)

Sirolimus concentration (• g l^{-1})	Precision (%)			Mean concentration (• g l^{-1})	Accuracy (%)
	Intra-	Inter-	Total		
0.2	10.3	3.1	10.8	0.206	103.0
0.5	7.5	4.2	8.6	0.476	95.2
20	7.5	1.1	7.6	19.6	98.0
50	9.2	2.2	9.4	48.1	96.2

[a] Determined by the method of Krouwer and Rabinowitz [20].
[b] Accuracy• mean sirolimus concentration over weighed-in sirolimus concentration• 100%.

order to produce a suitable charged species, $[M \cdot NH_4]^+$, for mass spectrometric detection using selected reaction monitoring. Streit et al. [19] employed the sodium adduct, $[M \cdot Na]^+$, of sirolimus for mass spectrometric single ion monitoring. The sodium adduct of sirolimus was not suitable for selected reaction monitoring as it is more stable than the ammonium adduct and thus requires more energy to produce fragmentation. The resultant product ion spectra of the sodium adduct contains more fragmentation and thus give a less sensitive response for selected reaction monitoring than the sirolimus ammoniated species.

A comparison of our HPLC–ESI-MS–MS method with the single ion monitoring method of Streit et al. [19], in terms of assay performance, revealed some differences. Firstly, the smaller sample requirements for our method (500 • l cf. 1000 • l) and secondly, improved precision at low concentrations (inter-assay precision of 2.7% at 0.2 • $g\,l^{-1}$ cf. 19% at 1.0 • $g\,l^{-1}$). The improved performance of our method, compared to Streit et al., may be attributed to the increased selectivity of two successive mass filtrations used with selected reaction monitoring.

We have previously reported HPLC–ESI-MS–MS quantitative methods for tacrolimus [22,23], a structural analogue of sirolimus. As the chemical properties of these compounds are similar, we were able to adapt our tacrolimus solid-phase extraction method for sirolimus. One modification to our tacrolimus extraction method was the utilisation of 15 m*M* zinc sulphate in the precipitation reagent. This change produced a cleaner supernatant than that obtained without its use and thus solid-phase cartridges were not prone to partial or total blockage. The HPLC–MS method reported by Streit et al. [19] utilised a similar procedure with methanol-water saturated with zinc sulphate (70:30, v/v) as the precipitation reagent. Investigators reporting HPLC–UV methods have employed liquid–liquid extraction sample preparation (diethyl ether [15], *tert.* butylmethyl ether [16] and butyl chloride-diethyl ether [18]). Overall, the specificity of HPLC–ESI-MS–MS has allowed for a less intensive sample preparation compared to HPLC–UV methods.

The simple solid-phase extraction procedure and chromatographic analysis time of 10 min allows the processing of approximately 30 samples in an 8 h shift. Further, up to 72 samples can be analysed with a 24-h turnaround time, thus making this method suitable for therapeutic drug monitoring of sirolimus if required for its future clinical use. The ability to provide a 24-h turnaround time on reporting results fulfils the requirements of the Consensus guidelines of Yatscoff et al. [13].

For other immunosuppressant drugs (ie. cyclosporine and tacrolimus) which have required therapeutic drug monitoring, we have seen the development of immunoassays for the clinical laboratory [24,25]. Historically and appropriately the evaluation of such methods has been performed against a reference method [26,27]. As our reported method measures parent drug specifically and has acceptable accuracy and precision over the expected therapeutic range, this method should be considered a reference method as defined by Shaw et al. [28]. Thus our HPLC–ESI-MS–MS method for sirolimus would be suitable for the evaluation of any commercial immunoassays that may be developed.

In conclusion, the validated HPLC–ESI-MS–MS assay described provides an accurate and precise method for the quantification of sirolimus in whole blood over the range of 0.2 to 100.0 • $g\,l^{-1}$. The wide analytical range of this method makes it suitable for therapeutic drug monitoring and pharmacokinetic studies. Further, the method described is currently being used for quantification of sirolimus in Phase II and III clinical investigations of the drug in solid organ transplant recipients.

References

[1] C. Vézina, A. Kudelski, S.N. Sehgal, J. Antibiot. 28 (1975) 721.
[2] S.N. Seghal, H. Baker, C. Vézina, J. Antibiot. 28 (1975) 727.
[3] F.J. Dumont, M.J. Staruch, S.L. Koprak, M.R. Melino, N.H. Siga, J. Immunol. 144 (1990) 251.
[4] B.D. Kahan, J.Y. Chang, S.N. Seghal, Transplantation 52 (1991) 185.
[5] B.D. Kahan, S. Gibbons, N. Tejpal, S.M. Stepkowski, T.-C. Chou, Transplantation 51 (1991) 232.
[6] Y. Tu, S.M. Stepkowski, T.C. Chou, B.D. Kahan, Transplantation 59 (1995) 177.
[7] J. Fryer, R.W. Yatscoff, E.A. Pascoe, J. Thilveris, Transplantation 55 (1993) 340.
[8] G.M. Ferron, E.V. Mishina, J.J. Zimmerman, W.J. Jusko, Clin. Pharmacol Ther. 61 (1997) 416.

[9] C. Brattström, J. Säwe, G. Tydén, G. Herlenius, K. Claesson, J. Zimmerman, C.-G. Groth, Ther. Drug Monit. 19 (1997) 397.
[10] J. J Zimmerman, B.D. Kahan, J. Clin. Pharmacol. 37 (1997) 405.
[11] M. Sattler, F.P. Guengerich, C.-H. Yun, U. Christians, K.-F. Sewing, Drug Metab. Dispos. 20 (1992) 753.
[12] M. Spatzenegger, W. Jaeger, Drug Metab. Rev. 27 (1995) 397.
[13] R.W. Yatscoff, R. Boeckx, D.W. Holt, B.D. Kahan, D.F. LeGatt, S. Sehgal, S.J. Soldin, K. Napoli, C. Stiller, Ther. Drug Monit. 17 (1995) 676.
[14] R.W. Yatscoff, D. LeGatt, R. Keenan, P. Chackowsky, Transplantation 56 (1993) 1293.
[15] R.W. Yatscoff, C. Faraci, P. Bolingbroke, Ther. Drug Monit. 14 (1992) 138.
[16] K.L. Napoli, B.D. Kahan, J. Chromatog. B. 654 (1994) 111.
[17] K.L. Napoli, B.D. Kahan, Clin. Chem. 42 (1996) 1943.
[18] J.-O. Svensson, C. Brattström, J. Säwe, Ther. Drug Monit. 19 (1997) 112.
[19] F. Streit, U. Christians, H.-M. Scheibel, K.L. Napoli, L. Ernst, A. Linck, B.D. Kahan, K.-F. Sewing, Clin. Chem. 42 (1996) 1417.
[20] J.S. Krouwer, R. Rabinowitz, Clin. Chem. 30 (1984) 290.
[21] V.P. Shah, K.K. Midha, S. Dighe, I.J. McGilveray, J.P. Skelly, A. Yacobi, T. Layoff, C.T. Viswanathan, C.E. Cook, R.D. McDowall, K.A. Pittman, S. Spector, J. Pharm. Sci. 81 (1992) 309.
[22] P.J. Taylor, A. Jones, G.A. Balderson, S.V. Lynch, R.L.G. Norris, S.M. Pond, Clin. Chem. 42 (1996) 279.
[23] P.J. Taylor, N.S. Hogan, S.V. Lynch, A.G. Johnson, S.M. Pond, Clin. Chem. 43 (1997) 2189.
[24] R.W. Yatscoff, K.R. Copeland, C.J. Faraci, Clin. Chem. 36 (1990) 1969.
[25] F.C. Grenier, J. Luczkiw, M. Bergmann, S. Lunetta, M. Morrison, D. Blonski, K. Shoemaker, M. Kobayashi, Transplant. Proc. 23 (1991) 2748.
[26] P.J. Taylor, P. Salm, R.L.G. Norris, P.J. Ravenscroft, S.M. Pond, Ther. Drug Monit. 16 (1994) 526.
[27] P. Salm, P.J. Taylor, A. Clark, G.A. Balderson, A. Grygotis, R.L.G. Norris, S.V. Lynch, L.M. Shaw, S.M. Pond, Ther. Drug Monit. 19 (1997) 694.
[28] L.M. Shaw, T.M. Annesley, B. Kaplan, K.L. Brayman, Ther. Drug Monit. 17 (1995) 577.

REVIEWS Drug Discovery Today • Volume 12, Numbers 3/4 • February 2007

Promising therapeutic potential of drugs targeting mTOR pathway

Reviews • KEYNOTE REVIEW

Targeting mammalian target of rapamycin (mTOR) for health and diseases

Chi Kwan Tsang, Haiyan Qi, Leroy F. Liu and X.F. Steven Zheng

Department of Pharmacology and Cancer Institute of New Jersey (CINJ) Robert Wood Johnson Medical School, 675 Hoes Lane, Piscataway, NJ 08854 USA

The macrolide rapamycin is used clinically to treat graft rejection and restenosis. Mammalian target of rapamycin (mTOR) is a central controller of cellular and organism growth that integrates nutrient and hormonal signals, and regulates diverse cellular processes. New studies have linked mTOR to several human diseases including cancer, diabetes, obesity, cardiovascular diseases and neurological disorders. Recent data have also revealed that mTOR is involved in the regulation of lifespan and in age-related diseases. These findings demonstrate the importance of growth control in the pathology of major diseases and overall human health, and underscore the therapeutic potential of the mTOR pathway.

Introduction

Rapamycin is a macrolide that is produced by the bacterium *Streptomyces hygroscopicus*, which was discovered in a soil sample collected ~1970 from the Easter Island *Rapa Nui*, from where the name rapamycin is derived (Box 1). Rapamycin was developed initially by Ayerst as an antifungal agent, but was soon abandoned because of the immunosuppressive effect and rapamycin was largely forgotten during the next decade. In the 20 years following its discovery only a dozen or so papers related to rapamycin were published. However, in the early 1990s the field experienced a dramatic turn of fortune, spurred largely by studies on the mechanism of action of rapamycin and by identification of the drug target. The growth of rapamycin-related research also renewed clinical interests and, in addition to rapamycin, several rapamycin analogs have been synthesized and tested in clinical trials. In 1997 rapamycin was approved by the FDA as an anti-rejection drug for kidney transplants.

Entering the 21st century, the field has continued the explosive growth. Recent studies provide significant insights into the molecular architecture of the mammalian target of rapamycin (mTOR) pathway. More importantly, the role of the mTOR pathway as a key process that underlies many human diseases has been either discovered or confirmed. New clinical indications for rapamycin and rapamycin analogs keep arising, and the scope of these is beyond their immunosuppressive activity. Rapamycin and rapamycin analogs are in clinical trials for several conditions such as cancer and cardiovascular diseases. In 2003, the FDA approved the rapamycin-

Chi Kwan Tsang
Dr Tsang is a post-doctoral fellow in pharmacology at Robert Wood Johnson Medical School (RWJMS). He obtained his PhD from Kagoshima University in 2002.

Haiyan Qi
Dr Qi is an assistant professor of pharmacology. She received her PhD from New York Medical College in 1996 and post-doctoral training at Princeton University.

Leroy F. Liu
Dr Liu is a professor and Chairman of Pharmacology at RWJMS. His research area is in cancer therapeutics. Dr Liu is an associate editor for several leading cancer journals, including *Cancer Research*. He has received many awards and honors, including the Bruce F. Cain Memorial Award for Outstanding Preclinical Research by AACR in 1997.

X.F. Steven Zheng
Dr Zheng is University Professor of Pharmacology at RWJMS. He is a pioneer and expert in target of rapamycin (TOR) signaling and mechanism of rapamycin action. He currently serves on the editorial boards of *Drug Discovery Today* and *Translational OncoGenomics*. Drs Liu and Zheng are both supported by multiple NIH R01 grants.

Corresponding author: Zheng, X.F. Steven (zhengst@umdnj.edu)

A brief history of rapamycin

1970 Collected soil sample from Easter Island (Rapa nui) and isolated *S. hygroscopicus*
1975 Purified rapamycin as a natural compound from *S. hygroscopicus* and discovered its fungicidal activity
1977 Discovered immunosuppressive activity in animal models
1984 Discovered antitumor activity
1989 Proposed immunosuppressive action
1992 Identified rapamycin inhibits $p70^{S6K}$ in mitogenic pathway in mammals
1993 Isolated *TOR* gene from yeast
1994 Isolated *mTOR* gene
1995 Elucidated the mechanism of action of rapamycin
1997 FDA-approved for preventing host-rejection in kidney transplants
2003 FDA-approved for use in drug-eluting stent

eluting stent, a revolutionary coronary angioplastic procedure. The goal of this article is to comprehensively review the role of mTOR in the pathology of diverse diseases and areas that are related closely to human health. Detailed analyses of the clinical benefits and potential for the existing inhibitors of mTOR, and new therapeutic opportunities are also presented.

Inhibitors of mTOR: rapamycin and rapamycin derivatives

Rapamycin is the founding member of the family of mTOR inhibitors. Rapamycin includes two separated moieties, the TOR-binding and the FKBP12-binding regions. To be active biologically, rapamycin must form a ternary complex with mTOR and FKBP12, which is a cytosolic binding protein collectively called immunophilin. Therefore, rapamycin acts to induce the dimerization of mTOR and FKBP12. The formation of a rapamycin–FKBP12 complex results in a gain-of-function because the complex binds directly to mTOR and inhibits the function of mTOR and the mTOR-mediated signaling network. For example, rapamycin blocks interleukin 2 (IL-2)-mediated T-cell proliferation and activation, conferring an immunosuppressive effect that is useful in transplantation. In addition, rapamycin is being developed to treat autoimmune diseases such as idiopathic and lupus membranous nephropathy. Rapamycin is also a potent inhibitor of the proliferation of vascular smooth muscle (VSM) cells. Based on this property, rapamycin (Sirolimus®) was approved by the FDA in 2003 as an antirestenosis drug used in coronary-artery stents. The Development Therapeutic Branch of the National Cancer Institute (NCI) was one of the first to test rapamycin, finding that it has superior, broad antitumor activity in both *in vitro* and *in vivo* models. There are many on-going clinical trials of rapamycin against a broad range of malignancies, from childhood lymphoma (Phase I) to prostate cancer (Phase IV). Additionally, clinical trials in conditions such as autosomal-dominant polycystic kidney disease (ADPKD) are being conducted.

Because of the promising therapeutic potential of rapamycin, pharmaceutical companies started to develop rapamycin analogs in the late 1990s. Several rapamycin analogs have been synthesized to improve the pharmacokinetic properties and for patent protection. Figure 1 shows the main rapamycin analogs under development. Because rapamycin and these derivatives share the same mechanism of action, we refer to them collectively as rapamycins in this review. CCI779 (also called temsirolimus; Wyeth) was the earliest developed rapamycin analog. It is a more water-soluble ester derivative of rapamycin for intravenous and oral formulation. CCI779 has antitumor activity either alone or in combination with cytotoxic agents in several human cancer cell lines and mouse xenografts [1]. Phosphatase and tensin homolog deleted on chromosome ten (PTEN)-deficient human tumors appear to be particularly sensitive to growth inhibition by CCI779 [2]. RAD001, which is also called everolimus (Novartis), is a hydroxyethyl ether derivative of rapamycin that has been developed for oral administration. Preclinical results demonstrate that the immunosuppressive activity of RAD001 in preventing allograft rejection in experimental rat models is synergystic with cyclosporine, thereby reducing cyclosporine-associated renal toxicity [3]. Currently, this compound is undergoing Phase III and Phase IV clinical trials for transplantation in the USA, and has been approved by the European Agency for the Evaluation of Medicinal Products for renal and heart transplants. RAD001 also shows excellent activity against several human cancer cells *in vitro* and tumors in animal models, and antiangiogenic activity by inhibiting the proliferation of human vascular endothelial cells [4]. AP23573 (Ariad) is synthesized by substituting the C-43 secondary alcohol moiety of the cyclohexyl group of rapamycin with phosphonate and phosphinate groups. It retains high-affinity binding to FKBP12 and mTOR-inhibitory activity, is stable in organic solvents, aqueous solutions at various pHs, plasma and whole blood [5], and is being developed for either oral or intravenous administration. AP23573 inhibits the proliferation of diverse human tumor cell lines *in vitro* and of tumor xenografts in conjunction with cytotoxic agents [6], and clinical trials are evaluating its antitumor activity. In general, rapamycin analogs have similar therapeutic effects to rapamycin but with improved hydrophilicity and are suitable for both oral and intravenous administration.

Overall, rapamycins are tolerated well by humans. They do not exhibit the significant renal toxicity that occurs with the most common immunosuppressive drugs FK506 (tacrolimus) and cyclosporine. The immunosuppressive effects can be reduced significantly by intermittent administration of these mTOR inhibitors for the treatment of human cancer [7]. The primary side-effect of mTOR inhibitors in adult humans is a dose-dependent increase in serum cholesterol and triglycerides [8]. Other adverse effects are relatively mild, including skin reactions, muscositis, minimal myelosuppression and diarrhoea. Additionally, initial clinical studies show no significant changes in blood pressure, kidney function, such as glomerular filtration, and liver function.

mTOR and the mTOR signaling network

mTOR is a well-conserved 289 kDa phosphatidylinositol 3-kinase (PI 3-kinase)-related kinase (PIKK) that occurs in all eukaryotic organisms sequenced so far. The structural organization of mTOR is shown in Figure 2a. The C-terminal PIKK domain is conserved most highly and exhibits serine and threonine kinase activity but no lipid kinase activity as seen with other members of the PIKK family [9]. An intact PIKK domain is required for all known functions of TOR [10,11]. The FKBP12-rapamycin-binding (FRB) domain is an 11-kDa region near the PIKK domain [11,12]. FRB

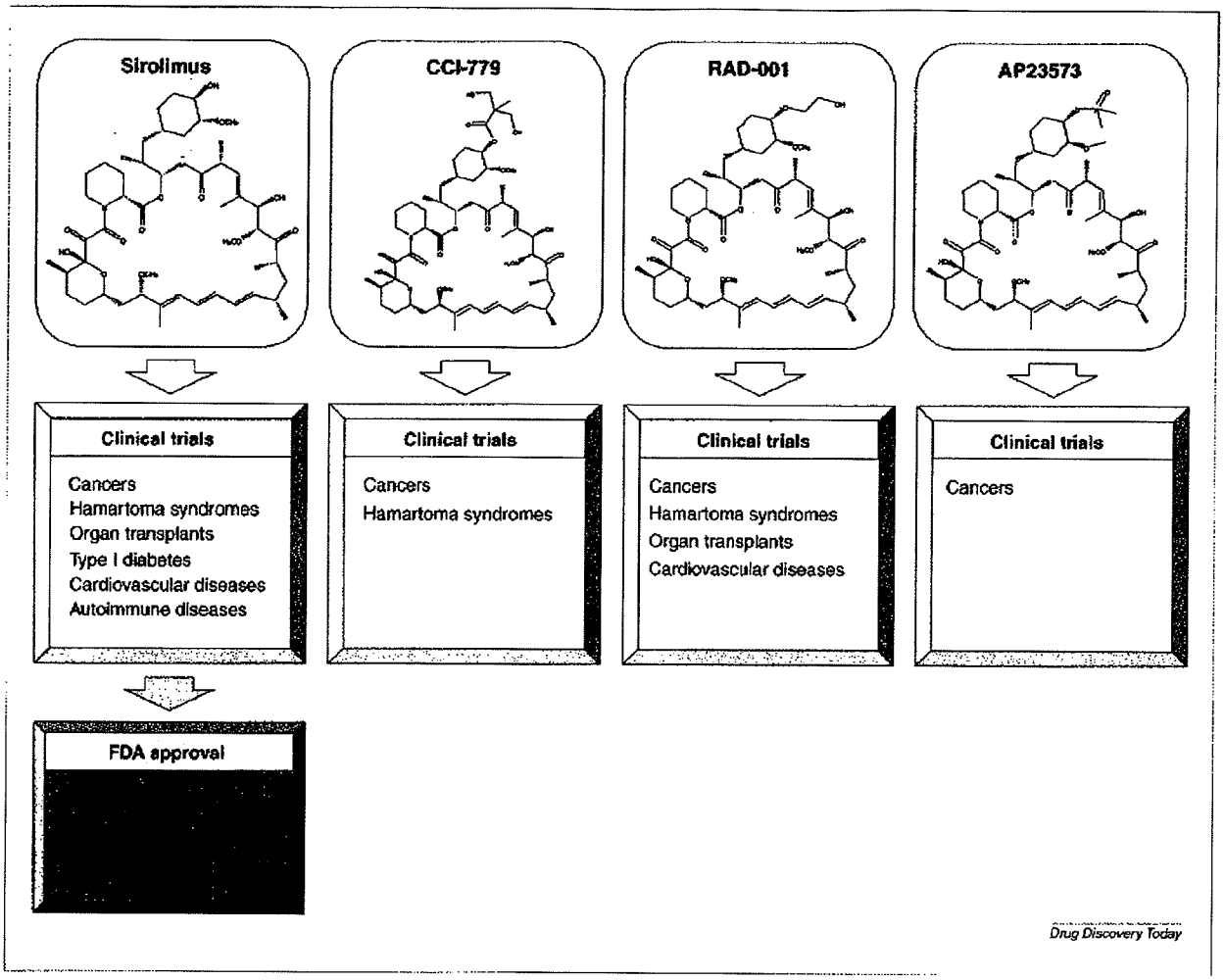

Clinical uses and trials of rapamycin and rapamycin analogs. Chemical structures, current clinical trials and FDA-approved clinical uses of rapamycin and its analogs.

forms a four-helical-bundle hydrophobic pocket that interacts with the hydrophobic rapamycin of FKBP12–rapamycin (Figure 2b) [13]. In effect, rapamycin binds FRB and FKBP12 to form a sandwich-like structure (Figure 2c). The FRB domain occurs only in the TOR protein, but not in other members of the PIKK family, which explains the unusually high specificity of rapamycin. Although the FRB domain is close to the PIKK domain, FKBP12–rapamycin does not appear to inhibit the catalytic activity of the kinase directly [11]. Therefore, how FKBP12–rapamycin interferes with the functions of mTOR remains elusive. One possibility is that FKBP12–rapamycin creates a spatial hindrance that prevents interaction between the PIKK domain and substrates that bind to the N terminus. The N terminus of TOR consists of ~20 tandem repeats of 37–43 amino acids, which are termed HEAT repeats [14]. Each HEAT unit contains two interacting α-helices and a flexible inter-helical spacer. Different HEAT units occur in tandem repeats and form super helices that are involved in interaction with other proteins. Indeed, TOR HEAT repeats interact with cofactors, such as mKog1/Raptor [15], and kinase substrates, such as Gln3 [16]. Recent studies have revealed that mTOR forms at least two distinct complexes. The mTOR complex 1 (mTORC1) is composed of mTOR, mLST8/GβL and Raptor, whereas mTORC2 consists of mTOR, mLST8/GβL, Rictor/mAvo3 and Sin1/mAvo1 [17]. Although mTORC1 is responsible for sensing nutrient signals, mTORC2 is involved in the organization of actin. In addition, mTORC2 is the Ser473 kinase for Akt/protein kinase B (PKB). FKBP12–rapamycin interacts with and inhibits mTORC1, but not mTORC2. Therefore, unless stated, our discussion relates to mTORC1, and the term mTOR refers to mTORC1.

Upstream of mTOR

mTOR is a central integrator of various extracellular and intracellular signals, including growth factors, nutrients, energy and stress (Figure 3). Among the signal inputs, growth factor- and hormone (e.g. insulin)-induced mTOR activation is the best characterized, and is mediated by the activation of PI 3-kinase. Active PI 3-kinase

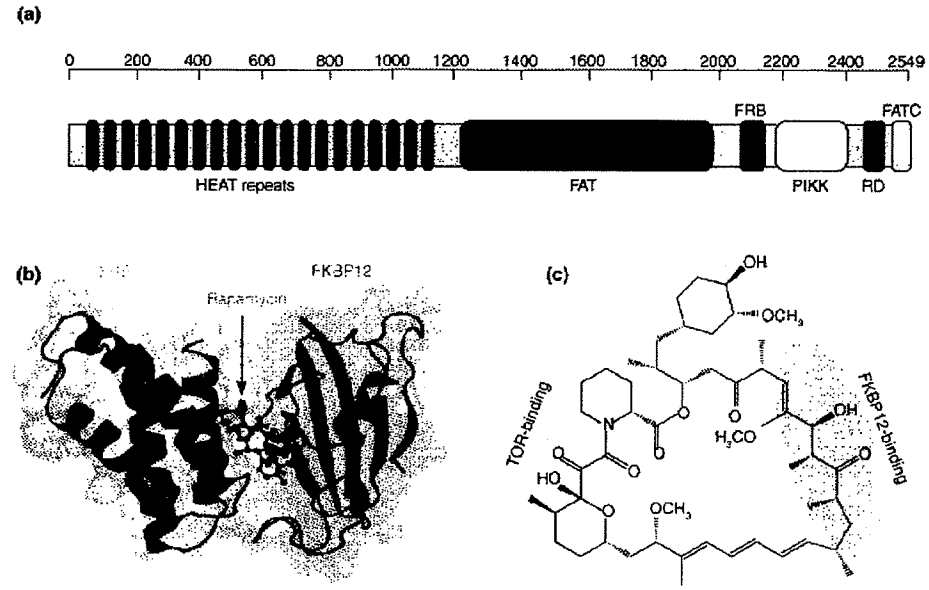

(a) Functional domains of mTOR: HEAT, huntington-elongation factor 1A-protein phosphatase 2A-A subunit-TOR; FAT, FRAP, ATM, TTRAP2; FRB, FKBP12 rapamycin binding; RD, regulatory domain; FATC, FAT, C terminal; and PIKK, PI 3-kinase-related kinase. The amino acid residue number (top) shows the relative positions of the domains. **(b)** The structure of the ternary complex of FRB (red), rapamycin (green) and FKBP12 (blue). Reprinted, with permission, from Choi *et al.* 1996, *Science* 273, 239–242 [13]. Copyright 2007 AAAS **(c)** Chemical structure of rapamycin and its binding sites for FKBP12 (blue region) and mTOR (red region).

localizes to the cell membrane and catalyzes the conversion of phosphatidylinositol (4,5)-biphosphate [PtdIns(4,5)P_2] into PtdIns(3,4,5)P_3, whose concentrations are regulated negatively by the tumor suppressor PTEN. PtdIns(3,4,5)P_3 recruits and activates Akt, which, in turn, phosphorylates and inactivates the tuberous sclerosis protein complex (TSC), which is a heterodimer composed of TSC1 and TSC2 [18]. TSC2 acts as a GTPase-activating protein (GAP) for the small GTPase Rheb, and the action of TSC is thought to be mediated by Rheb, possibly by the binding of Rheb to the kinase domain of mTOR, which activates mTOR in a GTP-dependent manner [19]. Several studies also show that GTP-loading of Rheb induces a conformational change in mTOR that results in activation of mTOR and phosphorylation of downstream effector proteins [19]. Other studies have shown that Akt might phosphorylate mTOR directly at Ser2448 [20], but the functional significance of phosphorylation of this remains to be established.

Nutrients represent another major signal input that activates mTOR. Unlike growth-factor-induced signaling, the exact mechanism of nutrient regulation of mTOR remains obscure, although the process is conserved evolutionarily from mammals to lower organisms such as *Saccharomyces cerevisiae*. One possibility is that nutrients regulate TOR signaling through energy production in the form of ATP. The cellular energy level (ATP:AMP ratio) is detected by AMP-activated protein kinase (AMPK). Under conditions of energy deprivation, the ATP:AMP ratio is low, which activates AMPK. Active AMPK phosphorylates TSC2 at multiple serine and threonine sites and activates TSC, which results in inactivation of mTOR [21]. Another study shows that the K_m of mTOR for ATP is high (mM range), which is close to the intracellular concentration of ATP. Based on this finding, it has been proposed that mTOR serves as a homeostatic sensor of ATP [22]. Various environmental stresses also lead to downregulation of mTOR signaling. For example, hypoxia inhibits mTOR and protein synthesis through two homologous proteins, REDD1 and REDD2 [23]. Upon hypoxia, both REDDs are upregulated by the transcription factor HIF1 and inhibit mTOR through TSC. DNA damage can also inhibit mTOR via p53 and the AMPK–TSC signaling pathway [24]. The regulation of TOR by stress is also conserved in lower eukaryotes. For example, inhibition of TOR by either rapamycin or disturbance of the plasma membrane activates the yeast stress-regulated mitogen-activated kinase Mpk1, which, in turn, phosphorylates silenced chromatin regulator 3 (Sir3) and leads to derepression of genes in otherwise silenced subtelomeric regions [25].

Downstream of mTOR

Growth and development require mTOR, and disruption of mTOR results in embryonic lethality and severe developmental defects [26]. At the cellular level, mTOR is central to the regulation of both catabolic and anabolic processes. In response to optimal growth stimuli, mTOR promotes the synthetic capabilities of the cell by upregulating key processes such as ribosome biogenesis and protein translation, which lead to an increase in cell mass and size, and, thus, accelerated proliferation. The best characterized downstream effectors of mTOR are the ribosomal protein S6 kinases (S6K) and 4E-BP1 (also called PHAS-I). S6K1 is phosphorylated

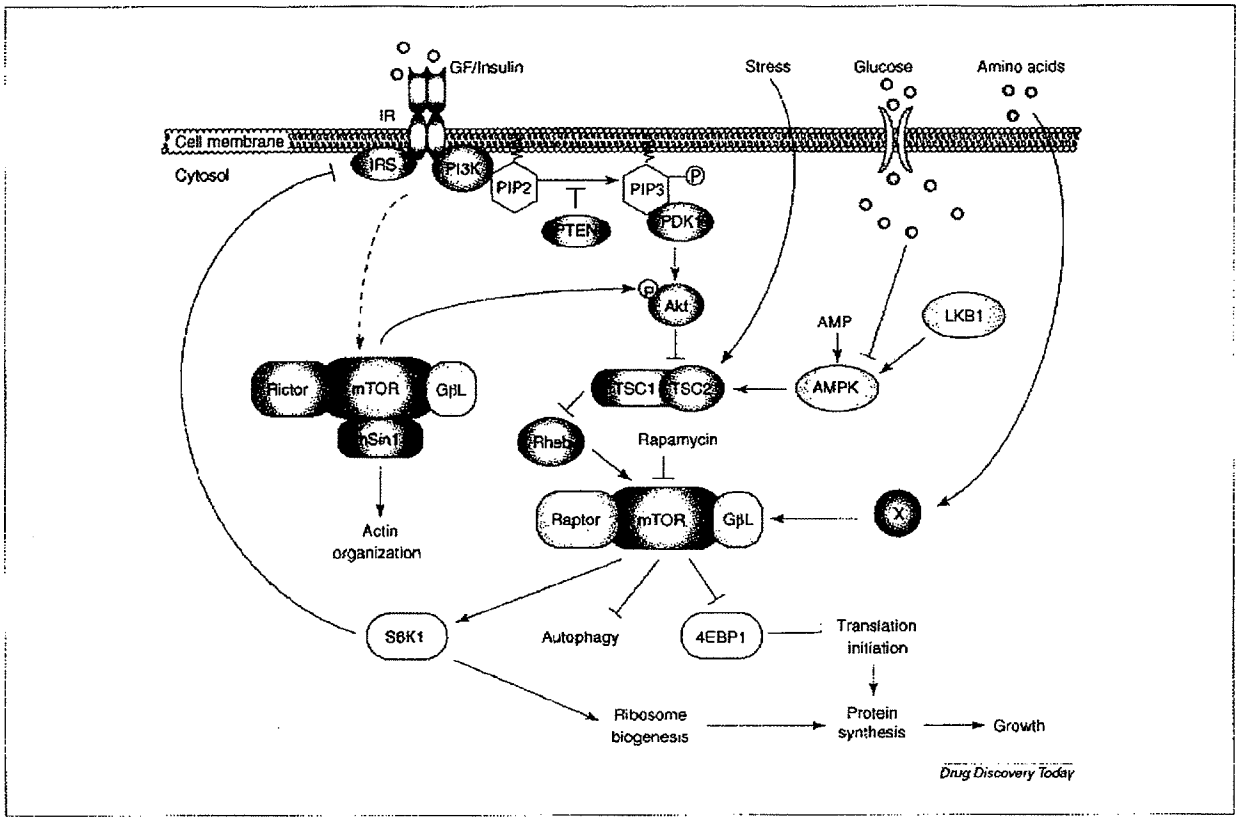

Signaling network of mTOR. mTOR integrates input signals from growth factors (GF), nutrients (glucose and amino acids) and stress to regulate cell growth via different cellular processes. Arrows and bars represent activation and inhibition, respectively. Protein X represents an unknown mediator.

directly by mTOR during stimulation with either nutrients or growth factors, which results in a selective increase in the translation of mRNA transcripts that contain a 5′ tract of oligopyrimidine (5′-TOP) motif [27]. The 5′-TOP mRNAs encode components of the translation apparatus such as elongation factors and ribosomal proteins. Thus, mTOR-dependent activation of S6K1 promotes an overall increase in protein synthesis. However, S6 phosphorylation and translation of 5′-TOP mRNAs are still responsive to mitogens in a rapamycin-dependent manner in a S6K1/S6K2 double-knockout mutant, which indicates that an alternative effector is also present [28]. 4E-BP1 is an inhibitor of eukaryotic translation initiation factor 4E (eIF4E). After hyperphosphorylation by mTOR, 4E-BP1 dissociates from eIF4E, which allows eIF4E to associate with the 5′-CAP of mRNAs and initiate translation [29]. Conversely, inhibition of mTOR by growth-factor withdrawal, nutrient starvation and stress conditions lead to downregulation of ribosome biogenesis, which is a high-energy-consuming process [30]. In addition, downregulation of the mTOR pathway also stimulates catabolic processes such as autophagy. Autophagy is a membrane-trafficking process that involves the delivery of cytoplasmic contents, such as organelles and macromolecules, to lysosomes/vacuoles, where the cytoplasmic contents are broken down to provide an intracellular supply of nutrients [31]. Autophagy is essential for adaptation and survival during starvation conditions. Autophagy has also been linked to tumorigenesis. It is further involved in the removal of large protein aggregates, the underlying pathological causes for several neurological disorders [31].

mTOR in health and disease

In the past 5 years, growth has been recognized as a central process in most, if not all, aspects of cell biology. An increasing number of human diseases have been linked to the dysregulation of mTOR, including immunological disorders, cancer, metabolic diseases, cardiovascular diseases and neurological disorders. Intriguingly, most of these are due to aberrant hyperactivity of the mTOR pathway, which makes inhibitors of mTOR potentially effective therapeutics for the treatment of these diseases. One of the most exciting developments is the finding that mTOR is a key regulator of lifespan in eukaryotes and contributes significantly to age-related diseases. The fact that rapamycin can extend lifespan in model organisms indicates that pharmacological modulation of aging is, potentially, a practical approach.

Allograft rejection and autoimmune disorders

Organ transplantation often elicits a complex series of immunological responses such as inflammation, which results in allograft rejection. After organ transplantation, the graft is recognized by T

cells as carrying foreign antigens through the interaction between MHC-antigen complex and T-cell receptor (TCR). Through an autocrine mechanism, such engagement leads to the production of IL-2, and IL-2-stimulated activation and proliferation of lymphocytes. Rapamycin, FK506 and cyclosporine, the widely used immunosuppressive agents after organ transplantation, have distinct mechanisms of action [32]. Their immunosuppressive activities require that they bind to specific cytosolic binding proteins, collectively called immunophilins. Cytosporine forms a complex with cyclophilin, whereas FK506, which is structurally related to rapamycin, forms complex with FKBP12. After forming a complex with their respective immunophilin, cyclosporine and FK506 inhibit the Ca^{2+}-dependent phosphatase calcineurin, thereby blocking T-cell antigen receptor-dependent expression of IL-2, which is a key cytokine in the proliferative response of T cells [33]. By contrast, rapamycin–FKBP12 binds to and inactivates mTOR, thereby preventing IL-2-stimulated T-cell proliferation [34]. Clinical trials in the late 1990s confirmed the efficacy of mTOR inhibitors as potent immunosuppressive agents in renal transplants. Combining rapamycin with a calcineurin inhibitor achieves significant synergy, lowering the dose of each drug that is needed for immunosuppressive efficacy, and improving the rejection prevention and minimizing cyclosporine-induced nephrotoxicity [35]. Rapamycin has neither the vasomotor renal-side effects of calcineurin inhibitors nor an increased risk of malignancy [36]. As a result, calcineurin inhibitor-replacement therapy, using rapamycin plus glucocorticoids and mycophenolate mofetil, has been developed for patients at risk of renal toxicity associated with calcineurin inhibitors [37]. Moreover, a side-effect of cyclosporine and tacrolimus might be diabetes, but clinical trials reveal no increased risk of post-transplantation diabetes in rapamycin-treated patients. However, it should be noted that, in a recent study, oral glucose-tolerance tests show that rapamycin is associated with a 30% increase in the incidence in impaired glucose tolerance in kidney-transplant recipients [38]. Thus, special attention should be paid to diabetic patients who need renal transplantation. Clinical trials for transplantation of other solid organs are underway.

Rapamycins have shown efficacy in several animal models of autoimmune diseases, including allergic encephalomyelitis, insulin-dependent diabetes mellitus, lupus and adjuvant arthritis [39]. In addition, autoimmune diseases are often associated with chronic inflammatory immune responses that are perpetuated by dendritic cells. mTOR is crucial for the survival of monocyte-derived dendritic cells [40]. Furthermore, rapamycin decreases surface concentration of some MHC class II molecules on murine bone marrow-derived dendritic cells, and inhibits their maturation [41]. These observations indicate that mTOR inhibitors might be therapeutically valuable in autoimmune disorders such as rheumatoid arthritis, psoriasis and multiple sclerosis. The efficacy of mTOR inhibitors in these autoimmune disorders is being investigated in several early clinical trials.

Cancer

Soon after the isolation and characterization of rapamycin in the early 1970s, it was shown to be a potent anticancer agent by the NCI. Initially, it was thought to inhibit the cell cycle because chronic treatment with rapamycin leads to G1 cell-cycle arrest.

TABLE 1

Components of the mTOR pathway involved in human cancers

Mutant protein	Clinical diseases and types of cancer
PTEN	Glioblastoma, prostate cancer, endometrial cancer
PI 3-kinase	Transformation, cancer
Akt	Breast cancer, chronic myeloid leukaemia, ovarian cancer
TSC1/2	Tuberous sclerosis
eIF4E	Lymphoma
S6K1	Breast cancer
NF1	Neurofibromatosis type 1, periphera nerve-sheath tumors
LKB1	Peutz-Jeghers syndrome, gastrointestinal hamartomas
P53	Tumors
4EBP	Transformations
Beclin-1	Breast carcinomas
HIF	Kidney cancer
Myc	Burkitt's lymphoma
Cyclin D1	Mantle cell lymphoma

However, it has been appreciated recently that growth is an important prerequisite for proliferation [19,42]; without sufficient cell mass and size, the cell cycle cannot be sustained and, eventually, cells become arrested in G1. Recent advances in cancer biology reveal that numerous human cancers, including lymphomas, melanomas, gliomas, malignancies of the CNS, and carcinomas of the lung, bladder, kidney, ovary, breast, prostate, stomach, pancreas, head and neck, contain mutations in genes that encode components of the mTOR signaling network [43]. These genetic abnormalities can cause hyperactivity of PI 3-kinase; overexpression of Akt, Rheb, eIF4E and S6Ks; either loss-of-function or deficiency of the tumor suppressors PTEN, TSC1/2 and LKB1, and underexpression of beclin-1 (Table 1), although a mutation of mTOR itself has not been reported. Consistent with these data, cancer cells in which mTOR becomes hyperactive because of either a mutation in *PTEN* or overexpression of *AKT* are particularly susceptible to rapamycins [2,44]. This provides the conceptual basis for the use of mTOR inhibitors to block the downstream pathways that are important for the growth of cancer cells, interrupting proliferation and accelerating apoptosis [45].

Rapamycins are undergoing active clinical trials to evaluate their antiproliferative action in cancer. Clinical trials have demonstrated their efficacy and mild side-effects. The most encouraging results of the anticancer effect of mTOR inhibitors have been obtained in renal cell carcinoma, mantle cell lymphoma (MCL) and endometric cancers. Compelling results have also been observed in refractory patients. Based on these promising results, CCI779 has been filed for registration in the USA and Europe for first-line treatment of patients with advanced renal cell carcinoma. More importantly, these clinical studies provided useful information on the types of cancer that might be more sensitive to mTOR inhibitors. For example, MCL and endometrial cancers have functional apoptosis pathways, and are usually accompanied by genetic mutations, such as loss of PTEN and overexpression of cyclin D1, that lead to aberrantly overactive mTOR-signal transduction. In such cases, they are likely to be more sensitive to rapamycin and apoptosis might be triggered by relatively low

doses of mTOR inhibitor. By contrast, some types of cancer, such as renal cell carcinoma and breast cancer, have either redundant signaling pathways or non-functional apoptosis pathways and so might require high doses of mTOR inhibitor to elicit a cytostatic response, and no dose-dependent apoptosis can be observed. However, as yet, it is not possible to predict accurately which cancer types are sensitive to mTOR inhibitors.

Another function of mTOR that is related to cancer development is tumor angiogenesis, the growth of blood vessels that provide tumor cells with nutrients and oxygen. The role of mTOR in tumor vascularization is interesting because preclinical studies have demonstrated that rapamycins have antiangiogenetic effects. Rapamycin lowers the concentration of vascular endothelial growth factor (VEGF), which leads to the suppression of endothelial-cell proliferation, survival and migration, and, eventually, tumor-vessel thrombosis [46]. It has been shown that the expression and function of hypoxia-induction factor (HIF) depends on mTOR [47]. Moreover, hypoxia also regulates mTOR in HIF-dependent and HIF-independent manners [48]. HIF-dependent inhibition of mTOR is mediated by upregulation of REDD1 and REDD2 [23]. Frequently, the hypoxia pathway is constitutively active in solid-tumor cells and, therefore, might be selectively reliant on mTOR for survival in hypoxic environments. Rapamycin treatment might cause apoptosis of hypoxic cancer cells that depend upon mTOR for survival, but not affect normal cells because they do not grow under these conditions. It is possible that the antiangiogenic effect of rapamycin is as important as growth inhibition in the suppression of solid tumors.

The direct and indirect effects of rapamycins on the growth of cancer cells make them excellent candidates for therapeutic agents in cancer. The hallmark of some cancers is the evasion of apoptosis. Thus, cancer cells occasionally become resistant to conventional chemotherapeutic agents, especially when the apoptotic regulator, such as Akt, is mutated. A recent finding using a murine lymphoma model shows that rapamycin reverses the chemoresistance that results from mutant Akt [44]. The important implications of this study are that induction of apoptosis by pharmacological inhibition of mTOR might restore drug sensitivity, and that combining conventional chemotherapy agents with rapamycin might be an important strategy to reverse drug resistance in human cancer.

A major challenge in rapamycin-based cancer therapy is to identify the right population of patients. Typically, ≤10% of patients respond to rapamycin. Some cancer cells are highly sensitive to rapamycin whereas others are significantly resistant. Most advances in research on the sensitivity of tumors to rapamycin have been made using cancers in which the PI 3-kinase–PTEN–AKT pathway is altered. However, the percentage of rapamycin-sensitive tumors that can be attributed to changes in PI 3-kinase–PTEN–AKT is unclear. Recently, some PTEN $^{-/-}$ tumors have been reported to be highly resistant to rapamycin [49]. Further investigation is needed to address these issues. A recent genomic screen of rapamycin sensitivity in yeast has identified mutations in many genes that affect rapamycin sensitivity [50], most of which are well conserved in humans. It will be interesting to determine whether either mutations or changes in expression of their human homologues have similar roles in cancer cells. The identification and treatment of molecularly defined patient cohorts, based on molecular phenotype, is a top priority for patient-orientated cancer therapy of mTOR-dependent cancers. Such studies would also provide important rationales for combinational therapy with rapamycin and other FDA-approved anticancer drugs. In addition, effective surrogate markers need to be developed to follow rapamycin-based therapy conveniently. Currently, most laboratory and clinical studies use phosphorylation of S6K1 to follow inhibition of mTOR. However, S6K1 is inhibited efficiently, even in cancer cells that are highly resistant to rapamycin. It is equally important to evaluate the combinational use of an mTOR inhibitor with other anticancer drugs to achieve maximal efficacy and minimal side-effects.

Diabetes

Diabetes is a metabolic disorder of glucose homeostasis. Insulin regulates blood-glucose levels by promoting the uptake and conversion of glucose to glycogen and its storage in the liver and muscles [51]. Insulin is produced by the β-cells in pancreatic islets. Type 1 diabetes is caused by loss of insulin production due to destruction of pancreatic β-cells. Currently, the only way to restore and sustain the normal concentration of blood glucose in patients with type 1 diabetes is either transplanting a pancreas or infusing isolated islets. Clinical studies using immunosuppressive regimens that contain rapamycin to prevent the rejection of islet transplants have shown significant efficacy in type 1 diabetic patients [52]. Thus, the use of rapamycins is crucial in the treatment of type 1 diabetes. By contrast, mTOR has a positive role in the growth of pancreatic β cells [53]. Acting downstream of PI 3-kinase–Akt, mTOR mediates insulin-induced protein translation and proliferation of 3 cells. In addition, glucose and branched amino acids stimulate β-cell growth in an mTOR-dependent manner [55]. This role of mTOR is supported further by the phenotype of mice deficient in S6K1, a kinase that acts downstream of mTOR. The S6K1 $^{-/-}$ mice have smaller islets, are hypoinsulinaemic and glucose intolerant [54]. These mice have a sharp reduction in glucose-induced insulin secretion and in pancreatic insulin content because of a selective decrease in β-cell size. Thus, the opposing effects of mTOR inhibitors must be balanced carefully in islet transplantation.

Type 2 diabetes arises when insulin secretion from pancreatic β cells fails to compensate for the peripheral insulin resistance (or insensitivity to insulin) in skeletal muscle, liver and fat cells [55]. Evidence indicates that insulin resistance might be caused by inhibition of insulin-receptor substrate (IRS) proteins by phosphorylation, which abolishes the signal transduction from insulin receptor to PI 3-kinase [51]. Although many distinct pathways have been implicated in downregulating IRS function, recent data indicate that sustained activation of mTOR signaling is a crucial event that renders IRS irresponsive to insulin [56]. Moreover, it has been demonstrated that rapamycin restores the sensitivity of IRS to insulin. Because mTOR is downstream of the IRS–PI3K–Akt pathway, the reported mTOR-mediated inhibition of IRS is thought to act via a negative-feedback loop [56]. Furthermore, it has been demonstrated that S6K1 phosphorylates IRS directly, which results in the inhibition of the association of IRS with the insulin receptor [57]. Another recent finding indicates that chronic hyperglycemia can lead to chronic activation of mTOR in β-cells [58]. Chronically active mTOR triggers phosphorylation

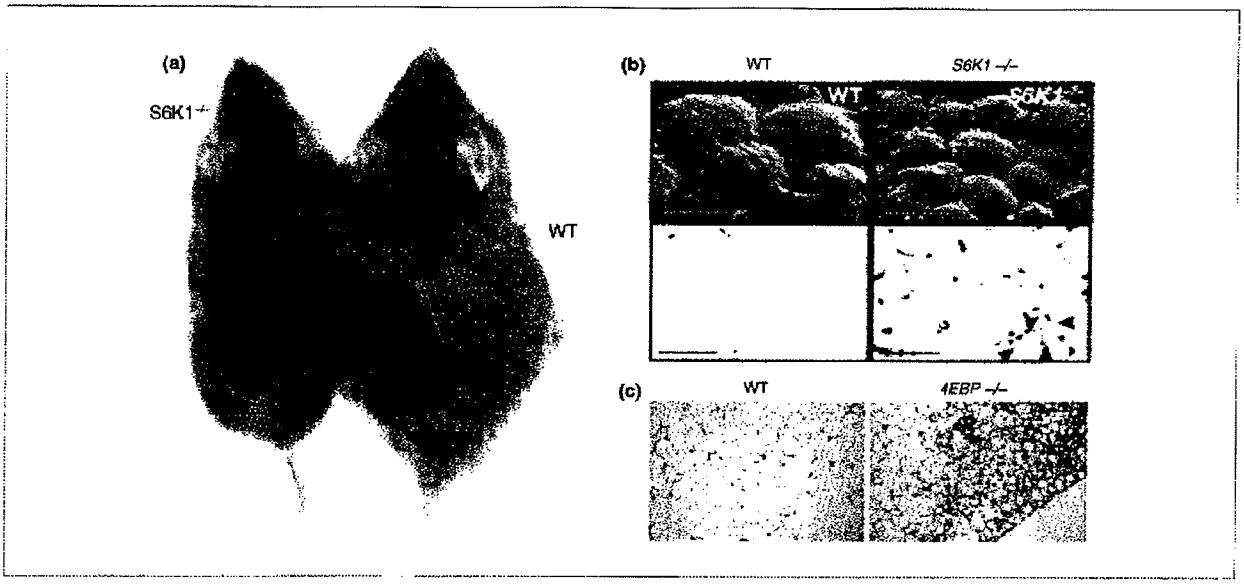

Regulation of mTOR-mediated fat accumulation and metabolism. (a) Wild-type (WT) and S6K1$^{-/-}$ mice after 6 months on a high-fat diet. **(b)** Scanning electron microscopic (upper panel) and histological (lower panel) analyses of epididymal white adipose tissue of wild-type and S6K1$^{-/-}$ mice. Reprinted, with permission, from McMillan Publishers Ltd: Um *et al.* 2004, *Nature* 431, 200–205 [65], copyright 2007. Arrowhead indicates multilocular adipocytes. Magnification for scanning microscopy and histology are 500× and 200×, respectively. **(c)** Retroperitoneal white adipose tissue of wild-type and 4EBP$^{-/-}$ mice. Sections stained with HandE. Reprinted, with permission, from McMillan Publishers Ltd: Tsukiyama–Kohara *et al.* 2001, *Nature Med.* 7, 1128–1132 [66], copyright 2007.

and subsequent proteosomal degradation of IRS2, which leads to an increase in β-cell apoptosis. Together, these studies indicate that persistent activation of mTOR in insulin-responsive cells downregulates insulin signaling and contributes to insulin resistance; whereas, persistent activation of mTOR in β-cells reduces cell mass and insulin secretion. Both situations can increase the risk of type 2 diabetes. Therefore, rapamycin is potentially useful in management of type 2 diabetes.

Obesity

According to the American Heart Association, >60% of Americans are either overweight or obese, which creates serious problems in healthcare and the overall economy. Understanding the cause of obesity and finding effective prevention and treatment methods are paramount tasks. Accumulating evidence indicates that mTOR has a role in lipid metabolism. During adipogenesis, the expression of mTOR increases dramatically, from barely detectable in preadipocytes to highly expressed in fully differentiated adipocytes [59,60], and rapamycin inhibits adipocyte differentiation [61]. Moreover, mTOR is required for the expression and activity of peroxisome proliferator-activated receptor-γ, a transcription factor that is crucial for adipogenesis [59,60]. Lipin, a lipodystrophy and obesity protein, is another possible target of mTOR. Phosphorylation of lipin is stimulated by insulin and amino acids in a rapamycin-sensitive manner [62]. Adipose tissue is not only for storing fat, it is also responsible for the secretion of hormones that regulate appetite. Leptin is a protein hormone that is synthesized predominantly by adipocytes and acts on receptors in the CNS and other sites to inhibit food intake and promote energy expenditure. mTOR regulates the synthesis and secretion of leptin from adipose cells [63]. Thus, by regulating leptin production in adipocytes, mTOR might have a broader role in controling whole-body energy metabolism.

Experiments in fruit flies indicate that TOR is required for fat accumulation, which further supports the notion that fat accumulation and metabolism are regulated by activity of mTOR [64]. It has been suggested that the regulation of mTOR-mediated fat metabolism involves signaling through S6K1 and 4E-BP1. More direct evidence of the role of the mTOR–S6K1 pathway in fat metabolism has been obtained from the S6K1-mutant mice. In these mice, high-fat diet- and age-dependent obesity is reduced markedly (Figure 4A,B), possibly because of the lower amounts of adipose tissue and fat accumulation that result from higher β-oxidation of fatty acids (lipolysis) in adipocytes [65]. Reduction of adipose tissue is also observed in mice that lack the translational inhibitor 4E-BP1 (Figure 4C) [66]. These observations indicate that S6K1 and 4E-BP1 might be novel therapeutic targets for the development of antiobesity drugs.

Cardiovascular diseases

Cardiac hypertrophy (heart enlargement) is caused by abnormally large cardiomyocytes. Cardiac hypertrophy accompanies many forms of heart disease, including ischemic disease, hypertension, valvular disease and heart failure. At the cellular level, cardiac hypertrophy is characterized by an increase in cell size and enhanced protein synthesis [67]. Although there are various hypertrophic stimuli, such as neurohormones and peptide growth factors, and several protein kinase cascades are involved in cardiac hypertrophy, it is likely that all forms of hypertrophic stimuli activate the general protein translational machinery in an mTOR-

dependent manner. Remarkably, inhibition of mTOR by rapamycin prevents cardiac hypertrophy in numerous transgenic mouse models. In addition, stress-induced cardiac hypertrophy is dependent on mTOR in mice [68]. These results indicate that mTOR is crucial for the abnormal cardiac overgrowth, and that mTOR inhibitors are promising agents for treatment of human cardiac hypertrophy.

Since the first surgery of percutaneous transluminal angioplasty in 1977, coronary intervention has led to the successful treatment of patients with narrowing of the coronary arteries [69]. Traditional balloon angioplasty and the stents that were developed later have been used widely to unblock and widen the affected arteries. However, after angioplasty, the artery often narrows again (a phenomenon called restenosis) because of vessel recoil or/and the overgrowth of scar tissue on the artery wall. Although insertion of a stent eliminates the vessel-recoil problem and is, therefore, a big improvement over balloon angioplasty, restenosis still occurs in many patients because of overgrowth of VSM cells. This is because the interaction between blood components and the metal surface of the stent stimulates proliferation of VSM cells. To circumvent this issue, drug-eluting stents have been developed to inhibit the growth of VSM cells [70]. Rapamycin (sirolimus)-coated stents effectively reduce restenosis and have been approved by the FDA [70]. The proposed mechanism of inhibition of proliferation of VSM cells by rapamycin involves inactivation of S6K1, impairment of Rb phosphorylation, and prevention of p27 down-regulation [70]. Additionally, studies *in vitro* show that rapamycin inhibits platelet-derived growth factor-induced migration of human VSM cells without affecting their cytoskeletal components and ability to bind collagen [71].

Neurological functions and disorders

Recent findings show that mTOR inhibitors might treat some human neurological disorders such as Huntington's, Alzheimer's and Parkinson's diseases. Because rapamycins are hydrophobic, they pass through the blood–brain barrier, making them attractive drug candidates in treating the aforementioned diseases and brain tumors. Huntington's disease is a neurodegenerative condition caused by a mutant form of huntingtin with abnormally long glutamine repeats at the N terminus. The mutant protein accumulates as intraneuronal aggregates that are thought to cause nerve cell damage and toxicity, possibly by interacting with and disrupting the transcriptional activity of several transcription factors. Rapamycin attenuates the accumulation of huntingtin and cell death, and protects against neurodegeneration in animal models of Huntington's disease [72]. Moreover, rapamycin induces an autophagy response that has been suggested to play a role in the 'clearance' of huntingtin aggregates. Similar large-protein aggregates occur in other neurodegenerative disorders such as aggregation of the insoluble β-amyloid in the brain of Alzheimer's patients. Thus, the rapamycin-induced autophagy response might help to remove and degrade β-amyloid in Alzheimer's patients. Interestingly, several reports indicate that mTOR might also be linked to Alzheimer's disease through translation of tau mRNA and degradation of tau protein [73]. The tau protein is found frequently in the brains of Alzheimer's patients, and is thought to contribute to the formation of neurofibrillary tangles. In a fly model, it has been demonstrated that rapamycin reduces the concentration of tau and lowers the toxicity caused by tau accumulation [74]. Therefore, mTOR inhibitors might be useful in preventing the accumulation of toxic tau protein in Alzheimer's patients.

As mentioned previously, mTOR signaling has a role in the response to stress. Under stressful conditions such as oxidative insult, mTOR signaling is inhibited, which results in the induction of some stress-responsive genes. One such stress-induced gene, which is involved in oxidative response in yeast is *YDR533C* [75]. Mutation of the human homolog, *DJ-1*, is associated with autosomal recessive, early-onset Parkinson's disease [76]. It is postulated that inhibition of mTOR might induce the expression of *DJ-1* and so protect neurons in Parkinson's patients. There is also evidence that tuberous sclerosis complex (TSC) mutations cause neuropsychiatric disorders such as epilepsy, mental retardation and autism [77]. The neuropathology of TSC is probably due to developmental abnormalities of the cerebral cortex, including missing normal six-layered structure of the cortex, dysmorphic neurons, large astrocytes and a unique type of cell known as a giant cell [78]. As the major downstream effector of TSC proteins, mTOR might also be associated with TSC-mediated neuropsychiatric disorders, and the therapeutic inhibition of mTOR might benefit these diverse neurological diseases.

In addition to being involved in neurological disorders, mTOR is implicated in the normal function of the CNS. Learning and memory are achieved by long-term synaptic plasticity, often called long-term potentiation (LTP) in mammals and long-term facilitation (LTF) in the marine snail *Aplysia*. Long-term changes in synaptic function and structure are confined to the stimulated synapses and require the local synthesis of proteins from pre-existing mRNAs. mTOR and translational components are enriched at postsynaptic sites [79] and both localized protein synthesis and the induction of LTP/LTF are inhibited by rapamycin [80]. These findings demonstrate that mTOR controls synaptic protein synthesis, and indicate that mTOR has a positive role in learning and memory, and in brain function in general.

Regulation of lifespan and aging

The world is facing a rapid expansion of an aging population. Aging is characterized as a progressive accumulation of functional impairments in organs and tissues, leading to increased risk of diseases and death. Age-related diseases and lifespan are two important readouts of aging. Recently, studies using model organisms such as yeast, worms, fruit flies and mice have identified key genetic and environmental factors in aging. Many genes that affect longevity were discovered in *Caenorhabditis elegans*. Among them, genes that are involved in the insulin or insulin-like growth factor (IGF) signaling pathway have attracted much attention. In *C. elegans*, mutations in the IGF1–PI3K pathway extend lifespan: mutation in *daf-2*, the insulin/IGF receptor results in a twofold increase in lifespan and mutation in *age-1*, the PI 3-kinase that acts downstream of *daf-2*, leads to 65% extension of lifespan. In *Drosophila*, mutation in either *dTOR* or its substrate *dS6K*, results in a longevity phenotype, and overexpression of *dTSC1* and *dTSC2*, which leads to inhibition of dTOR, also extends lifespan [81]. In yeast, extension of the replicative and chronological lifespan have also been observed as a consequence of mutations in the

TOR pathway [82,83]. Recent studies indicate that the role of the TOR pathway in lifespan regulation is conserved in mammals. For example, heterozygous deletion of the IGF receptor in mice extends lifespan by 26% [84], and polymorphisms in the genes that encode the IGF1 receptor and PI 3-kinase are linked with longevity in humans [85].

Lifespan can be also modified by the simple, non-genetic manipulation of caloric restriction (CR), which is a powerful method that enhances longevity in yeast, *C. elegans*, fruit flies, mice and other nonhuman mammals. Usually, CR is achieved by reducing the food intake by 30–40% of *ad libitum*, without compromising the supply of essential nutrients. This simple manipulation extends lifespan by 15–40%, and also delays the onset of age-related diseases [86]. CR leads to several physiological changes, including lower plasma concentration of insulin, lower body temperature, and decreased oxidative damage to proteins, DNA and lipids [87]. The molecular mechanism by which CR increases longevity is unclear. However, the IGF/TOR pathway appears to have a key role. First, CR reduces the plasma IGF-1 concentration [88]. Second, the lifespan of fruit flies and yeast subjected to CR is not increased further by mutations in the IGF/TOR pathway [82]. Finally, the role of the TOR pathway as cellular-nutrient sensor is consistent with the idea that it mediates the CR effect on lifespan.

Identification of the downstream effectors of the IGF/TOR pathway in lifespan regulation is an important future task. One possible mechanism is upregulation of autophagy as a result of TOR inhibition. siRNA knockdown of BEC-1, a protein that is involved in autophagy, suppresses the longevity phenotype of *daf-2* in *C. elegans* [89]. However, the lifespan of wild-type worms is not affected by autophagy deficiency. It is possible that autophagy plays a role in the aging of long-lived organisms, where clearance of damaged proteins and organelles is necessary to maintain the normal functions of organs. Another possible mechanism is upregulation of the anti-stress response. Mutation in *daf-16*, the gene that encodes the forkhead transcription factor in *C. elegans*, suppresses the longevity phenotype of *daf-2* mutation [90]. Daf-16 has been shown to cross-talk with the TOR pathway by affecting transcription of the Raptor ortholog daf-15, a presumed TORC1 component, providing more evidence that dTOR is involved [91]. The involvement of the TOR pathway in lifespan regulation, together with the effects of rapamycin on aged-related diseases such as cancer, obesity, type II diabetes mellitus, autoimmune diseases, cardiovascular diseases and neuronal degeneration diseases, demonstrate the possibility that pharmacological approaches might extend human lifespan and improve the quality of life.

Other diseases

Increasingly, mTOR is implicated in other, less well-known diseases. An interesting example is ADPKD, which is an inherited condition that frequently leads to renal failure. Most cases of ADPKD are caused by mutations in polycystin-1 (PC1). It was shown recently that the cytoplasmic tail of PC1 interacts with tuberin, which results in inappropriate activation of the mTOR pathway in the epithelial cells that line the cysts in the kidneys of humans with ADPKD and in mouse models [92]. Rapamycin is effective in reducing renal cystogenesis in mouse models and the size of polycystic kidneys in human ADPKD patients after receiving a transplant. Phase I/II clinical trials are ongoing for rapamycin-treatment of ADPDK patients.

Discovery of new inhibitors of mTOR

A major challenge is to identify and understand the long-term negative effects of mTOR inhibitors. Although rapamycin and the currently available rapamycin analogs are well tolerated, their side-effects are not documented fully. Nevertheless, because mTOR is involved in many cellular processes and disease pathways, selective inhibitors that target a subset of mTOR-regulated functions are likely to reduce the undesirable side-effects. By contrast, many tumors are not very responsive to rapamycin therapy, the mechanism of which is still unclear. Conceivably, an agent that disrupts both mTOR complexes is likely to be a more potent anticancer drug. In addition, new rapamycin derivatives might have improved pharmacological properties and/or reduced production costs.

Three rapamycin analogs, namely CCI779, RAD001 and AP23573, have been designed and manufactured for development as anticancer and immunosuppressive drugs. There is an on-going effort to identify additional rapamycin analogs with pharmacological improvements over rapamycin, reduced production costs, minimized side-effects, and to study SARs. Usually, drug analogs are generated by synthetic methods, semi-synthetic methods, precursor feeding and biosynthetic engineering. Recent advances in the area of rapamycin biosynthesis have shown promise for novel rapamycin analogs. For example, precursor-directed biosynthesis has been evaluated by feeding alternative rapamycin-precursor molecules to *Streptomyces hygroscopticus*. During rapamycin biosynthesis, L-lysine is converted to L-pipecolate, which is then incorporated into the molecule just before the final closure of the macrocyclic ring. It has been demonstrated that (±)-nipecotic acid enhances the incorporation of pipecolate analogs into rapamycin, leading to the production of two new sulfur-containing rapamycin analogs, 20-thiarapamycin and 15-deoxo-19-sulfoxyl-rapamycin [93]. Because rapamycin is synthesized via a mixed polyketide synthase–nonribosomal peptide synthetase enzymatic complex, genetic engineering of these polyketide synthases of *S. hygroscopticus* is a potential route for generating novel rapamycin analogs. Such a combinatorial biosynthesis method has produced a library of rapamycin analogs with altered oxidation and alkylation patterns. Moreover, exogenous carboxylic acids can be used to increase the diversity through mutasynthesis of the engineered rapamycin-producing strains for novel rapamycin analogs [94,95]. This approach has the advantage of rapid generation of many rapamycin analogs for SAR analysis and drug discovery.

Another approach, SAR by nuclear magnetic resonance spectroscopy, has been used to identify structurally simplified analogs of FK506 (the immunosuppressive compound that is structurally related to rapamycin) that bind to FKBP12 with high affinity [96]. This technology seems to be particularly useful in target-directed drug research and might be applied in the high-throughput screening of natural-product libraries for therapeutic analogs of rapamycin. Computational database screening such as Ludi has also been used as a tool to assist the *de novo* design of FKBP12 ligands and SAR studies, resulting in the identification of the simplified analog of FK506 [97]. This might represent an alternative approach for finding rapamycin analogs with tractable synthetic routes that block mTOR

function. With respect to modification of rapamycin itself, there is little room to improve the potency because rapamycin is already a potent inhibitor of mTOR. Nevertheless, rapamycin can be optimized further: for example, a hydroxyl group on carbon 43 of rapamycin is unstable because of its intrinsic metabolic site, and a carbonyl group on carbon 15 is important for FKBP12 binding [98]. Optimization of these sites might improve the stability and pharmacokinetic properties of the drug.

Of the two distinct mTOR complexes, mTORC1 and mTORC2, only mTORC1 is sensitive to inhibition by rapamycin [17]. A recent study reported that chronic rapamycin treatment also affects mTORC2, and it suggested that inhibition of mTORC2 is more important for the anticancer effect of rapamycin in some tumors [99]. The PIKK kinase domain of mTOR appears to be crucial for the function of both mTORC1 and mTORC2 [100]. Therefore, targeting the PIKK domain is likely to lead to more potent inhibitors of mTOR for cancer therapy. Recently, Shokat and colleagues synthesized a series of isoform-selective inhibitors of the PI 3-kinase family and defined the structural basis for their specificity [101]. They also assayed systematically the activity of these compounds on different members of the PI 3-kinase family. One of the compounds, PtdIns-103 has dual specificity for mTOR and PI 3-kinase α [102]. When used in a mouse model of malignant glioma, PtdIns-103 has excellent antitumor activity. However, one major concern is that inhibition of both mTOR complexes might have considerable toxicity. However, PtdIns-103 has no detectable side-effects, which indicates that the kinase-inhibitor approach is feasible.

Recent advances in the understanding of the molecular interactions between the components of the mTOR pathway provide excellent opportunities for developing novel inhibitors of this pathway. For example, stable association of mTOR with several proteins, including GβL/mLST8 and raptor/mKog1, is important for the function of mTOR [17]. It is conceivable that targeting these proteins might provide effective, alternative approaches for the development of new drugs. More recently, a study has demonstrated that farnesylthiosalicyclic acid promotes the dissociation of raptor and mTOR, and decreases phosphorylation of S6K1 in breast cancer cells [103], which demonstrates that this approach is feasible. It is estimated that, on average, each human kinase phosphorylates ~20 substrates. Although mTOR is known to control diverse cellular processes, only two proteins (4E-BP1 and S6K1) have been shown convincingly to be direct substrates of mTOR. More efforts are needed to identify substrates of mTOR, which are instrumental to understanding the overall growth regulatory functions of mTOR. Each substrate tends to be involved in a subset of mTOR-regulated processes and, thus, either one or a subset of diseases, so targeting mTOR substrates is likely to generate more-specific, small-molecule compounds. For example, mice that lack either S6K1 or 4E-BP1 prevent high fat diet- and age dependent obesity (Figure 4) [65,66]. Conceivably, these proteins might be used to screen for small molecules that might prevent and/or treat obesity.

Future perspective and conclusions

We have experienced amazing advances in the understanding of mTOR signaling during the past 15 years. This basic research has inspired clinical studies that reveal crucial roles of mTOR in a range of human disorders. Further research on mTOR will generate new understanding of how cells control their functions, with growth as the centerpiece. They will also reveal molecular details of how malfunctions at various steps lead to disease states, through genetic and/or environmental changes. Inhibitors of mTOR have already been shown to be well-tolerated, effective therapeutics in several disease areas (organ transplantation and drug-eluting stent). The future looks even brighter for mTOR inhibitors, many of which are either already in clinical trials (e.g. cancer) or have been implicated as useful therapeutic agents. We anticipate that the existing inhibitors of mTOR will have a much greater role in managing many major human diseases. Understanding the precise role of mTOR in regulating human aging and neurodegeneration are of paramount importance in helping with the health issues associated with an aging society. Although mTOR inhibitors are undergoing clinical trials to evaluate their effects in organ transplantation and inhibiting cancer cell growth, their potential to treat obesity, diabetes and neurological disorders are far behind on the clinical-development track. Evaluation of the clinical efficacy of mTOR inhibitors in these age-related diseases will have a long-lasting impact on society.

Acknowledgement

We apologize for being unable to cite all the relevant publications due to space constraint. Research in the authors' laboratories was supported by grants from the National Institutes of Health (L.F.L. and X.F.S.Z).

References

1 Yu, K. *et al.* (2001) mTOR, a novel target in breast cancer: the effect of CCI-779, an mTOR inhibitor, in preclinical models of breast cancer. *Endocr. Relat. Cancer* 8, 249–258

2 Neshat, M.S. *et al.* (2001) Enhanced sensitivity of PTEN-deficient tumors to inhibition of FRAP/mTOR. *Proc. Natl. Acad. Sci. U. S. A.* 98, 10314–10319

3 Schuurman, H. *et al.* (1997) SDZ RAD, a new rapamycin derivative: synergism with cyclosporine. *Transplantation* 64, 32–35

4 Vignot, S. *et al.* (2005) mTOR-targeted therapy of cancer with rapamycin derivatives 10.1093/annonc/mdi113. *Ann. Oncol.* 16, 525–537

5 Mita, M.M. *et al.* (2004) Phase I, pharmacokinetic (PK), and pharmacodynamic (PD) study of AP23573, an mTOR inhibitor, administered IV daily X 5 every other week in patients (pts) with refractory or advanced malignancies. *ASCO Meeting Abstracts* 22 (Suppl. 14), 3076

6 Clackson, T. *et al.* (2003) Broad anti-tumor activity of ap23573, an mTOR inhibitor in clinical development, *ASCO Annual Meeting* Abstract No: 882

7 Raymond, E. *et al.* (2004) Safety and pharmacokinetics of escalated doses of weekly intravenous infusion of CCI-779, a novel mTOR inhibitor, in patients with cancer. *J. Clin. Oncol.* 22, 2336–2347

8 Murgia, M. *et al.* (1996) The side effect profile of sirolimus: a phase I study in quiescent cyclosporine-prednisone-treated renal transplant patients. *Kidney Int.* 49, 209–216

9 Keith, C.T. and Schreiber, S.L. (1995) PIK-related kinases: DNA repair, recombination, and cell cycle checkpoints. *Science* 270, 50–51

10 Brown, E.J. *et al.* (1995) Control of p70 s6 kinase by kinase activity of FRAP *in vivo*. *Nature* 377, 441–446

11 Zheng, X.F. *et al.* (1995) TOR kinase domains are required for two distinct functions, only one of which is inhibited by rapamycin. *Cell* 82, 121–130

12 Chen, J. *et al.* (1995) Identification of an 11-kDa FKBP12-rapamycin-binding domain within the 289-kDa FKBP12-rapamycin-associated protein and

characterization of a critical serine residue. *Proc. Natl. Acad. Sci. U. S. A.* 92, 4947–4951
13 Choi, J. *et al.* (1996) Structure of the FKBP12–rapamycin complex interacting with the binding domain of human FRAP. *Science* 273, 239–242
14 Andrade, M.A. and Bork, P. (1995) HEAT repeats in the Huntington's disease protein. *Nat. Genet.* 11, 115–116
15 Kim, D. *et al.* (2002) mTOR interacts with raptor to form a nutrient-sensitive complex that signals to the cell growth machinery. *Cell* 110, 163–175
16 Bertram, P.G. *et al.* (2000) Tripartite regulation of Gln3p by TOR, Ure2p and phosphatases. *J. Biol. Chem.* 275, 35727–35733
17 Abraham, R.T. (2002) Identification of TOR signaling complexes: more TORC for the cell growth engine. *Cell* 111, 9–12
18 Inoki, K. *et al.* (2002) TSC2 is phosphorylated and inhibited by Akt and suppresses mTOR signaling. *Nat. Cell Biol.* 4, 648–657
19 Inoki, K. *et al.* (2005) Signaling by target of rapamycin proteins in cell growth control. *Microbiol. Mol. Biol. Rev.* 69, 79–100
20 Nave, B.T. *et al.* (1999) Mammalian target of rapamycin is a direct target for protein kinase B: identification of a convergence point for opposing effects of insulin and amino-acid deficiency on protein translation. *Biochem. J.* 344, 427–431
21 Inoki, K. *et al.* (2003) TSC2 mediates cellular energy response to control cell growth and survival. *Cell* 115, 577–590
22 Dennis, P.B. *et al.* (2001) Mammalian TOR: A homeostatic ATP sensor. *Science* 294, 1102–1105
23 Brugarolas, J. *et al.* (2004) Regulation of mTOR function in response to hypoxia by REDD1 and the TSC1/TSC2 tumor suppressor complex. *Genes Dev.* 18, 2893–2904
24 Feng, Z. *et al.* (2005) The coordinate regulation of the p53 and mTOR pathways in cells. *Proc. Natl. Acad. Sci. U. S. A.* 102, 8204–8209
25 Ai, W. *et al.* (2002) Regulation of subtelomeric silencing during stress response. *Mol. Cell* 10, 1295–1305
26 Gangloff, Y.-G. *et al.* (2004) Disruption of the Mouse mTOR Gene Leads to Early Postimplantation Lethality and Prohibits Embryonic Stem Cell Development. *Mol. Cell. Biol.* 24, 9508–9516
27 Dufner, A. and Thomas, G. (1999) Ribosomal S6 kinase signaling and the control of translation. *Exp. Cell Res.* 253, 100–109
28 Pende, M. *et al.* (2004) S6K1−/−/S6K2−/− Mice exhibit perinatal lethality and rapamycin-sensitive 5′-terminal oligopyrimidine mRNA translation and reveal a mitogen-activated protein kinase-dependent S6 kinase pathway. *Mol. Cell. Biol.* 24, 3112–3124
29 Lawrence, J. and Brunn, G. (2001) Insulin signaling and the control of PHAS-I phosphorylation. *Prog. Mol. Subcell. Biol.* 26, 1–31
30 Tsang, C.K. and Zheng, X.F.S. (2004) Control of ribosome biogenesis by target of rapamycin (TOR). *Recent Res. Dev. Mol. Cell Biol.* 5, 135–147
31 Shintani, T. and Klionsky, D.J. (2004) Autophagy in health and disease: a double-edged sword. *Science* 306, 990–995
32 Schreiber, S.L. and Crabtree, G.R. (1995) Immunophilins, ligands, and the control of signal transduction. *Harvey Lect.* 91, 99–114
33 Ho, S. *et al.* (1996) The mechanism of action of cyclosporin A and FK506. *Clin. Immunol. Immunopathol.* 80, S40–S45
34 Abraham, R. and Wiederrecht, G. (1996) Immunopharmacology of rapamycin. *Annu. Rev. Immunol.* 14, 483–510
35 Kahan, B. (1998) Emerging strategies for the clinical application of rapamycin. *Clin. Biochem.* 31, 341–344
36 Morales, J. *et al.* (2002) Sirolimus does not exhibit nephrotoxicity compared to cyclosporine in renal transplant recipients. *Am. J. Transplant.* 2, 436–442
37 Stegall, M. *et al.* (2003) Kidney transplantation without calcineurin inhibitors using sirolimus. *Transplant. Proc.* 35 (3 Suppl), 125S–127S
38 Teutonico, A. *et al.* (2005) Glucose metabolism in renal transplant recipients: effect of calcineurin inhibitor withdrawal and conversion to sirolimus. *J. Am. Soc. Nephrol.* 16, 3128–3135
39 Burkhardt, H. and Kalden, J. (1997) Xenobiotic immunosuppressive agents: therapeutic effects in animal models of autoimmune diseases. *Rheumatol. Int.* 17, 85–90
40 Woltman, A.M. *et al.* (2001) Rapamycin induces apoptosis in monocyte- and CD34-derived dendritic cells but not in monocytes and macrophages. *Blood* 98, 174–180
41 Hackstein, H. *et al.* (2003) Rapamycin inhibits IL-4–induced dendritic cell maturation *in vitro* and dendritic cell mobilization and function *in vivo*. *Blood* 101, 4457–4463
42 Richardson, C. *et al.* (2004) PI3-kinase and TOR: PIKTORing cell growth. *Semin. Cell Dev. Biol.* 15, 147–159
43 Guertin, D. and Sabatini, D. (2005) An expanding role for mTOR in cancer. *Trends Mol. Med.* 11, 353–361
44 Wendel, H. *et al.* (2004) Survival signalling by Akt and eIF4E in oncogenesis and cancer therapy. *Nature* 428, 332–337
45 Huang, S. and Houghton, P. (2003) Targeting mTOR signaling for cancer therapy. *Curr. Opin. Pharmacol.* 3, 371–377
46 Guba, M. *et al.* (2002) Rapamycin inhibits primary and metastatic tumor growth by antiangiogenesis: involvement of vascular endothelial growth factor. *Nat. Med.* 8, 128–135
47 Treins, C. *et al.* (2002) Insulin stimulates hypoxia-inducible factor 1 through a phosphatidylinositol 3-kinase/target of rapamycin-dependent signaling pathway. *J. Biol. Chem.* 277, 27975–27981
48 Hudson, C.C. *et al.* (2002) Regulation of hypoxia-inducible factor 1[alpha] expression and function by the mammalian target of rapamycin. *Mol. Cell. Biol.* 22, 7004–7014
49 Sarbassov, D.D. *et al.* (2006) Prolonged rapamycin treatment inhibits mTORC2 Assembly and Akt/PKB. *Mol. Cell* 22, 159–168
50 Chan, T.-F. *et al.* (2000) A chemical genomics approach toward understanding the global functions of the target of rapamycin protein (TOR). *Proc. Natl. Acad. Sci. U. S. A.* 97, 13227–13232
51 Saltiel, A. and Kahn, C. (2001) Insulin signalling and the regulation of glucose and lipid metabolism. *Nature* 414, 799–806
52 Shapiro, A.M.J. *et al.* (2000) Islet transplantation in seven patients with type 1 diabetes mellitus using a glucocorticoid-free immunosuppressive regimen. *N. Engl. J. Med.* 343, 230–238
53 McDaniel, M.L. *et al.* (2002) Metabolic and autocrine regulation of the mammalian target of rapamycin by pancreatic [beta]-cells. *Diabetes* 51, 2877–2885
54 Pende, M. *et al.* (2000) Hypoinsulinaemia, glucose intolerance and diminished [beta]-cell size in S6K1-deficient mice. *Nature* 408, 994–997
55 Rhodes, C.J. (2005) Type 2 diabetes-a matter of beta-cell life and death? *Science* 307, 380–384
56 Shah, O. *et al.* (2004) Inappropriate activation of the TSC/Rheb/mTOR/S6K cassette induces IRS1/2 depletion, insulin resistance, and cell survival deficiencies. *Curr. Biol.* 14, 1650–1656
57 Harrington, L.S. *et al.* (2004) The TSC1-2 tumor suppressor controls insulin-PI3K signaling via regulation of IRS proteins. *J. Cell Biol.* 166, 213–223
58 Briaud, I. *et al.* (2005) Insulin receptor substrate-2 proteasomal degradation mediated by a mammalian target of rapamycin (mTOR)-induced negative feedback down-regulates protein kinase b-mediated signaling pathway in [beta]-cells. *J. Biol. Chem.* 280, 2282–2293
59 Kim, J.E. and Chen, J. (2004) Regulation of peroxisome proliferator-activated receptor-[gamma] activity by mammalian target of rapamycin and amino acids in adipogenesis. *Diabetes* 53, 2748–2756
60 Cho, H. *et al.* (2004) Regulation of adipocyte differentiation and insulin action with rapamycin. *Biochem. Biophys. Res. Commun.* 321, 942–948
61 Yeh, W. *et al.* (1995) Rapamycin inhibits clonal expansion and adipogenic differentiation of 3T3-L1 cells. *Proc. Natl. Acad. Sci. U. S. A.* 92, 11086–11090
62 Huffman, T.A. *et al.* (2002) Insulin-stimulated phosphorylation of lipin mediated by the mammalian target of rapamycin. *Proc. Natl. Acad. Sci. U. S. A.* 99, 1047–1052
63 Fox, H.L. *et al.* (1998) Amino acids stimulate phosphorylation of p70S6k and organization of rat adipocytes into multicellular clusters. *Am. J. Physiol. Cell Physiol.* 274, C206–C213
64 Teleman, A. *et al.* (2005) Drosophila Melted modulates FOXO and TOR activity. *Dev. Cell* 9, 271–281
65 Um, S. *et al.* (2004) Absence of S6K1 protects against age- and diet-induced obesity while enhancing insulin sensitivity. *Nature* 431, 200–205
66 Tsukiyama-Kohara, K. *et al.* (2001) Adipose tissue reduction in mice lacking the translational inhibitor 4E-BP1. *Nat. Med.* 7, 1128–1132
67 Frey, N. *et al.* (2004) Hypertrophy of the heart: a new therapeutic target? *Circulation* 109, 1580–1589
68 McMullen, J.R. *et al.* (2004) Inhibition of mTOR signaling with rapamycin regresses established cardiac hypertrophy induced by pressure overload. *Circulation* 109, 3050–3055
69 Gruntzig, A. *et al.* (1979) Nonoperative dilatation of coronary-artery stenosis: percutaneous transluminal coronary angioplasty. *N. Engl. J. Med.* 301, 61–68
70 Serruys, P.W. *et al.* (2006) Coronary-artery stents. *N. Engl. J. Med.* 354, 483–495
71 Poon, M. *et al.* (1996) Rapamycin inhibits vascular smooth muscle cell migration. *J. Clin. Invest.* 98, 2277–2283
72 Ravikumar, B. *et al.* (2004) Inhibition of mTOR induces autophagy and reduces toxicity of polyglutamine expansions in fly and mouse models of Huntington disease. *Nat. Genet.* 36, 585–595
73 Li, X. *et al.* (2005) Levels of mTOR and its downstream targets 4E-BP1, eEF2, and eEF2 kinase in relationships with tau in Alzheimer's disease brain. *FEBS J.* 272, 4211–4220

74 Berger, Z. *et al.* (2006) Rapamycin alleviates toxicity of different aggregate-prone proteins. *Hum. Mol. Genet.* 15, 433–442

75 de Nobel, H. *et al.* (2001) Parallel and comparative analysis of the proteome and transcriptome of sorbic acid-stressed *Saccharomyces cerevisiae*. *Yeast* 18, 1413–1428

76 Bonifati, V. *et al.* (2003) Mutations in the DJ-1 gene associated with autosomal recessive early-onset Parkinsonism. *Science* 299, 256–259

77 Crino, P.B. and Henske, E.P. (1999) New developments in the neurobiology of the tuberous sclerosis complex. *Neurology* 53, 1384–1390

78 Goodman, M. *et al.* (1997) Cortical tuber count: A biomarker indicating neurologic severity of tuberous sclerosis complex. *J. Child Neurol.* 12, 85–90

79 Asaki, C. *et al.* (2003) Localization of translational components at the ultramicroscopic level at postsynaptic sites of the rat brain. *Brain Res.* 972, 168–176

80 Tang, S.J. *et al.* (2002) A rapamycin-sensitive signaling pathway contributes to long-term synaptic plasticity in the hippocampus. *Proc. Natl. Acad. Sci. U. S. A.* 99, 467–472

81 Kapahi, P. *et al.* (2004) Regulation of lifespan in *Drosophila* by modulation of genes in the TOR signaling pathway. *Curr. Biol.* 14, 885–890

82 Kaeberlein, M. *et al.* (2005) Regulation of yeast replicative life span by TOR and Sch9 in response to nutrients. *Science* 310, 1193–1196

83 Powers, R.W., 3rd *et al.* (2006) Extension of chronological life span in yeast by decreased TOR pathway signaling. *Genes Dev.* 20, 174–184

84 Holzenberger, M. *et al.* (2003) IGF-1 receptor regulates lifespan and resistance to oxidative stress in mice. *Nature* 421, 182–187

85 Bonafe, M. *et al.* (2003) Polymorphic variants of insulin-like growth factor I (IGF-I) receptor and phosphoinositide 3-kinase genes affect IGF-I plasma levels and human longevity: cues for an evolutionarily conserved mechanism of life span control. *J. Clin. Endocrinol. Metab.* 88, 3299–3304

86 Masoro, E.J. (2003) Subfield History: caloric restriction, slowing aging, and extending life. *Sci. Aging Knowledge Environ.* 2003, RE2

87 Gredilla, R. and Barja, G. (2005) Minireview: the role of oxidative stress in relation to caloric restriction and longevity. *Endocrinology* 146, 3713–3717

88 Breese, C.R. *et al.* (1991) Influence of age and long-term dietary restriction on plasma insulin-like growth factor-1 (IGF-1), IGF-1 gene expression, and IGF-1 binding proteins. *J. Gerontol.* 46, B180–B187

89 Melendez, A. *et al.* (2003) Autophagy genes are essential for dauer development and life-span extension in *C. elegans*. *Science* 301, 1387–1391

90 Lin, K. *et al.* (1997) daf-16: An HNF-3/forkhead family member that can function to double the life-span of *Caenorhabditis elegans*. *Science* 278, 1319–1322

91 Jia, K. *et al.* (2004) The TOR pathway interacts with the insulin signaling pathway to regulate *C. elegans* larval development, metabolism and life span. *Development* 131, 3897–3906

92 Shillingford, J.M. *et al.* (2006) From the Cover: The mTOR pathway is regulated by polycystin-1, and its inhibition reverses renal cystogenesis in polycystic kidney disease. *Proc. Natl. Acad. Sci. U. S. A.* 103, 5466–5471

93 Ritacco, F.V. *et al.* (2005) Production of novel rapamycin analogs by precursor-directed biosynthesis. *Appl. Environ. Microbiol.* 71, 1971–1976

94 Lowden, P. *et al.* (2004) New rapamycin derivatives by precursor-directed biosynthesis. *ChemBioChem* 5, 535–538

95 Gregory, M. *et al.* (2004) Isolation and characterization of pre-rapamycin, the first macrocyclic intermediate in the biosynthesis of the immunosuppressant rapamycin by *S. hygroscopicus*. *Angew. Chem. Int. Ed. Engl.* 43, 2551–2553

96 Shuker, S.B. *et al.* (1996) Discovering high-affinity ligands for proteins: SAR by NMR. *Science* 274, 1531–1534

97 Babine, R.E. *et al.* (1995) Design, synthesis and X-ray crystallographic studies of novel FKBP-12 ligands. *Bioorg. Med. Chem. Lett.* 5, 1719–1724

98 Gregory, D. *et al.* (1991) Atomic structure of the rapamycin human immunophilin FKBP-12 complex. *J. Am. Chem. Soc.* 113, 7433–7434

99 Sarbassov, D.D. *et al.* (2006) Prolonged rapamycin treatment inhibits mTORC2 assembly and Akt/PKB. *Mol. Cell* 22, 159–168

100 Zheng, X. *et al.* (1995) TOR kinase domains are required for two distinct functions, only one of which is inhibited by rapamycin. *Cell* 82, 121–130

101 Knight, Z.A. *et al.* (2006) A pharmacological map of the PI3-K family defines a role for p110[alpha] in insulin signaling. *Cell* 125, 733–747

102 Fan, Q.-W. *et al.* (2006) A dual PI3 kinase/mTOR inhibitor reveals emergent efficacy in glioma. *Cancer Cell* 9, 341–349

103 McMahon, L.P. *et al.* (2005) Farnesylthiosalicylic acid inhibits mammalian target of rapamycin (mTOR) activity both in cells and *in vitro* by promoting dissociation of the mTOR-raptor complex. *Mol. Endocrinol.* 19, 175–183